University of Nairobi

College of Architecture and Engineering

Institute of Nuclear Science and Technology

Distribution of normalized relative strontium in the femur of an adult Kenyan population

by

Agata Wilson Okong'o

S56/64410/2010

BEd. Science (Hons)

A thesis submitted in partial fulfillment for the degree of Master of Science in Nuclear Science in the Institute of Nuclear Science and Technology in the University of Nairobi

Declaration

This thesis is my original work and has not been presented for a degree in any other university.

Signature: …… Date:……..
Agata, Wilson Okong'o

Supervisors' Approval

This thesis has been submitted for examination with our knowledge as university supervisors.

Professor Michael J. Gatari (PhD) Signature: .....
Institute of Nuclear Science and Technology Date: .....
College of Architecture & Engineering
University of Nairobi

Professor Julius A. Ogeng'o (PhD) Signature: .....…
Department of Human Anatomy Date: .....
College of Biological and Physical Sciences
University of Nairobi

Dedication

This work is dedicated to my parents, Mr. and Mrs. Zedekiah N. Agata, who sacrificed beyond measure to ensure I got a decent and disciplined upbringing and education. I also dedicate it to my wife, Mercy Okong'o, for her unwavering moral support.

Acknowledgements

I wish to thank the almighty God for his blessings resulting in my successful completion of this study.

I acknowledge the kind and valuable support from my supervisors, Prof. M. J. Gatari and Prof. J. A Ogeng'o, that was much needed throughout the study period.

I am most grateful to the director, Institute of Nuclear Science & Technology (INST), Mr. D. M. Maina; Mr. M. Mang'ala, Lecturer at INST; Mr. S. Bartilol, Senior Technologist INST and the entire staff and student fraternity at the INST, University of Nairobi, for their unwavering support during the study.

I am indebted to the department of human anatomy at the University of Nairobi for their support in partly preparing and delivering the samples.

I appreciate the National Council for Science and Technology (NCST) for partly financing the study and International Science Programme (ISP) at Uppsala University, Sweden, for supporting INST with research instrumentation.

Table of Contents

List of tables

List of figures

List of Abbreviations

AAS – Atomic Absorption Spectrometry

ADC – Analogue to Digital Converter

BMC – Bone Mineral Content

BMD – Bone Mineral Density

BMI – Body Mass Index

DEXA – Dual Energy X – ray Analysis

DXA – Dual X – ray Analysis

EDXRF – Energy Dispersive X – ray Fluorescence

ICP – AES – Inductively Coupled Plasma – Atomic Emission Spectrometry

INST – Institute of Nuclear Science and Technology

JEE – JEOL – A vacuum evaporator system

MCA – Multichannel Analyser

PIXE – Proton Induced X – ray Emission

PSA – Power Spectrum Analysis

PXRF – Polarized X ray Fluorescence

SAXS – Small Angle X ray Scattering

SEM – Scanning Electron Microscope

SOTI – Spinal Osteoporosis Therapeutic Intervention

STRATOS – Strontium Ranelate for the Treatment of Osteoporosis

TROPOS – Treatment of Peripheral Osteoporosis

UON – University of Nairobi

XRD – X ray Diffraction

XRF – X ray Fluorescence

List of Definitions

Arthritis –The painful inflammation of joints accompanied by swelling and stiffness, (Fries, Spitz, Kraines, & Holman, 1980).

Camebax electron microprobe – An instrument designed for quantitative microanalysis using both energy and wavelength dispersive X ray spectrometry, (Reed, 1997).

Caucasian – Refers to people of the European descent with usually light skin pigmentation, (Jordan & Cooper, 2002).

Condyles – Rounded protuberance at the end of some bones that enables articulation with a different bone, (Kent, 2006).

Cortical bone – The dense bone that is made of organic ground substance and inorganic salts, (Bayraktar et al., 2004). It encompasses the marrow cavity.

Diaphysis – Shaft or central part of a bone, (Lenart, Lorich, & Lane, 2008).

Gait analysis - A specimen analysis technique that uses two force plates and a light source spot measuring device that consists of light emitting diodes with optoelectronic cameras, (Wada et al., 2001).

Hologic Software – A software used to predict fracture incidences based of bone densitometry, (Nissen et al., 2005).

Igneous rock – Rocks formed above or underground when magma gets trapped in small pockets, (Kirkpatrick, 1981).

Iliac bone – Uppermost and largest/widest bone of the pelvis, (Ahlmann, Patzakis, Roidis, Shepherd, & Holtom, 2002).

Lattice – A periodic arrangement of molecules or ions in a crystallite solid, (Isaacs, 1996).

Leeching – Subjected to terrestrial annelid worms, (Yantis, O'Toole, & Ring, 2009).

Monte Carlo simulations – Involve computational algorithms that solve problems by generating random numbers and observing which ones obey some property or properties, (Hammersley, Handscomb, & Weiss, 1965).

Osteomalacia - A bone mineral disorder that results in the weakening or softening of bones. This is sometimes called rickets in children, (Parfitt, 1990).

Osteoporosis - A bone condition that results in porous bones with high fracture incidences, (Kanis, Melton, Christiansen, Johnston, & Khaltaev, 1994).

Phallanges – These are bones that hold the finger tissues, (Landsmeer, 1949).

Photometer – A device that measures the intensity of light of a particular source against a known standard, (Rieke et al., 2004).

Placebo – A sham or an ineffective medicine or procedure given or administered as a control or to raise a patient's expectation (Stewart-Williams & Podd, 2004).

Proximal femur- The part of the femur that is located towards the center of the body, (Manninger & Kazár, 2007).

Ranelate – A strontium compound consisting of ranelic acid, (J. Reginster, 2002).

Resorption - The process whereby osteoclasts of a bone break it down thereby releasing minerals such as calcium into the blood stream, (Teitelbaum, 2000).

Supplemental escherichia coli phytase – A member of the histidine acid phosphatase family which has the highest specific activity of all general phytases, (Lim, Golovan, Forsberg, & Jia, 2000).

Trabecular bone – This is also called the cancellous or spongy bone or the porous part of a healthy bone, (Huiskes, Ruimerman, Van Lenthe, & Janssen, 2000).

Transiliac bone – Bone matter that extends from one iliac crest to another, (Cohen et al., 2010).

Abstract

Elemental density has a determinant role in bone mineral disorders like osteoporosis and osteopetrosis. Studies in bone elemental density show that other elements exist in bones besides the predominant element, Ca. Recent studies report that relative Sr (to Ca) can be used to treat bone disorders by preventing resorption of Ca from bones into blood and by facilitating the generation of new bone units. Osteoporotic bones have been reported to be Sr deficient meaning that mapping out elemental distribution across bones could give an indication of areas of the bone that are strong or otherwise. Other studies outline the frequent breakage of the hip axis length of the femur in osteoporosis patients thereby suggesting a bone weakness of some sort. Osteoporosis prevalence rates and incidences have been reported to be the lowest in Africa by extrapolation studies but there was no bone matrix information to aid in explaining this or compare with known relative Sr values from other world populations.

There is contradictory information on the nature of the relationship between bone morphometric parameters and bone mineral density. Some studies report a correlation between mass and length of bones with the bone mineral density while others report the opposite. These observations generated the need to know the distribution of relative Sr in human bones against the established threshold for normal bones hence provide vital information and clarifications for the reported inconsistencies stemming from other studies. This kind of assessment had not been carried out in Kenya at the time the main study took place yet bone mineral disorders did exist within the Kenyan population. The study was therefore the first in investigating the relative Sr distribution in selected cadaver femurs with respect to the abundant calcium and zinc.

A representative sample of femurs was obtained from the Department of Human Anatomy at the University of Nairobi (UoN) having been boiled (femurs), macerated

and cleaned off from their tissues. These were taken to the department of Civil and Structural engineering, at UoN, where morphometric measurements were done. The length and mass of the femurs were measured using a tape measure and a weighing balance respectively. At the Institute of Nuclear Science and technology (INST) laboratory the samples were cleaned and dried using double distilled water and a hot air blower respectively. The femurs were then partitioned by labeling nine relatively equal partitions including the heads of the femurs and the condyles. A makeshift sample holding system was used to hold each femur such that the flattest part of an irradiation partition rested on the primary radiation source and detector which were part of a calibrated Energy dispersive X-ray Fluorescence (XRF) analysis system that was available at INST, UoN. This system comprised of a sample hold, primary radiation source, detector, associated electronics, a cooling system and a computer. Irradiation took 1800s per an irradiation partition ending up with a histogram of counts per second versus energies in keV. Analysis of X ray spectra by least iterative squares was used to extract net intensities of Ca, Sr and Zn. These elements were prominent in the femurs as could be seen from their net intensities on the raw data tables. The net intensities were proportional to the actual concentrations of elements in the samples which could not be fairly obtained due to the irregular surface of the bones and the absence of bona fide bone standards. As such, normalization of the net intensities using their molar masses was done so as to provide reliable data for comparative or distributive studies as was the case in the main study. The normalized net intensities were then analyzed using statistical techniques of simple averaging and correlations (including bivariate) basing on the expected result from each specific objective. In assessing the distribution of relative Sr across the femur, averages were calculated for similar partitions, for example the average net intensity for the head of the femur in the 16 femurs was determined. Differences between paired irradiation partitions, based on averaged results were then analyzed using bivariate correlations. Correlations between femur morphometric parameters and relative Sr relied on normalized net intensities that had been found by calculating the

average intensity for each of the sixteen femurs, from the nine irradiation partitions per femur, then compared with values for mass and length of the femurs.

It was observed that the Sr to Ca ratio was mostly homogenous across the femurs and the slight differences appeared to depend on the region and architecture of the bone. The proximal femur had the lowest Sr to Ca ratios compared to the distal femur. Porous regions had therefore more Sr to Ca ratios and vice versa. The results could explain the frequent breaking of the hip axis lengths of the femurs in osteoporotic women as there was comparatively less relative Sr at the proximal femur bearing in mind that studies had reported that relative Sr was a biomarker for bone strength. There was no significant correlation between the morphometric parameters of the femur and Sr to Ca ratios. This meant that the fracture of femurs, due to their morphometric properties, was based on other factors such as mechanical positioning and the relative stress yields or binding of zinc which as observed in this study, correlated with the mass and length of the femurs. Sr to Zn ratios also appeared to depend on the bone region, as there were different values for the femur condyles, the shaft and the distal femur. Further to this, the proximal femur showed higher Zn to Sr ratios compared to the distal femur. There were no correlations between Sr to Zn ratios and the mass or length of the femurs. Parallels were drawn with the correlation of Sr to Ca ratios and the morphometric parameter of the femur. The normalized net intensities for the prominent elements in the bone were further analyzed to include results for sum of Sr and Zn versus calcium. These (Sr+Zn and Ca) were plotted against the femur morphometric parameters where they showed no correlation with the morphometric parameters but an inverse relationship with each other. This meant that Sr or Zn substituted themselves with Ca in the femur probably depending on the anatomical site or function as there was more Sr or Zn across porous regions of the femur. Zn, as well, had been observed to be a bone growth and strength biomarker in some studies. These findings are important in mapping the regional bone strength of the femur, based on specific bone elements, and may be of use in osteology.

Chapter 1
Introduction

1.1 Background

There was interest in studying Sr in bones due to an increased prevalence of osteoporosis and osteoporotic fractures. Research showed that Sr could be used as a drug for treatment and prevention of bone mineral disorders like osteoporosis and arthritis, which are both associated with Sr deficiency. A study by Meunier et al. (2004) at 72 centers in 11 European countries and Australia, observed that metabolic bone disorders such as osteoporosis had been associated with low concentrations of Sr in bone. According to Pines and Lederer (1947), cases where Sr concentration was high, disorders such as osteopetrosis were found to affect the bone. This showed that Sr was an important element in bone chemistry, which needed to be investigated for improving our knowledge of related bone disorders resulting from mineral density issues.

Bentley (2006) describes Sr (atomic number 38) as a soft silver white or yellowish metallic element that is chemically highly reactive. Consequently, it occurs naturally in compounds and it is the fifteenth most abundant element on earth (at 0.034 % of the average igneous rock). It is found in the form of sulfate mineral celestite and carbonate strontianite as observed by Suárez-Orduña, Rendón-Angeles, Lopez-Cuevas, and Yanagisawa (2004). Nilsson, Jensen, and Carlsen (1985) explain that Sr is present in soil, plants, water and in bones although in the latter it is in trace amounts. According to Johnson, Armstrong, and Singer (1968) Sr substitutes itself with calcium in bones since it has similar chemical and physical properties as Ca and this makes it to naturally seek the bone.

A method for quantifying Sr in human bones was designed by Pejovic, Stronach, Gyorffy, Webber, and Chettle (2004). The method involved x-ray florescence technology and was tested on phalanges and tibias of ten healthy subjects.

Measurements were done using a collimated ^{109}Cd radiation source positioned in 90^{o} alignment that sequentially included the source, the sample and the detector. Irradiation results showed statistically insignificant differences in the concentration of Sr between these bones. In this method, tissue attenuation and the geometry of sample placement were major sources of errors as the samples involved alive and healthy human beings. This study led to an interest of studying bones without tissues and on fixed geometry where no movement of the bones would arise as in the case of measurements on patients. Another study by Gedalia (1975) on fetal skeletons showed that Sr was mainly taken up by the bone during the time of bone and tooth formation. This study neither quantified nor investigated the distribution of relative Sr across the bones. Zamburlini et al. (2009) studied Sr depth distribution in the human bone using micro PIXE technology. They used five cadaver fingers of which they studied the cortical and trabecular bones. In their findings, Sr was evenly distributed across these bones in terms of depth. This study involved old male subjects thereby leaving an interest in studying bones from different sexes, different skeletal bones and bones from a variety of age groups.

1.2 Problem Statement

Current research shows that Sr influences the bone elemental density. Low Sr levels have been associated with bone disorders such as osteomalacia and osteoporosis while higher levels result in bone anomalies like osteopetrosis. Some studies have established a threshold/normal value for the quantity of relative Sr in human bones. In a Sr concentration study by Nielsen (2004) in human bones, the findings suggested Sr was averagely about 3.5 % of the Ca content in the bone while Dahl et al. (2001) reported between 0.01 to 0.03 % in sections of the western population. There is however no information on relative Sr distribution in human bones from an African geographical region, and more so in Kenya, from which skeletal averages could be worked out. Differences do exist though in terms of the soil, water and the human diet profile between Africa and the Western world. Research by Cooper,

Campion, and Melton (1992) shows that osteoporosis prevalence rates were different in the following regions: Scandinavia, North America, Southern Europe, Latin America and Asia. Schwartz et al. (1999) observed a difference in the hip fracture incidences among the following areas: Beijing and Hong Kong in China, Budapest in Hungary, Porto, parts of Brazil and Reykjavik Iceland. This suggests there could be a difference of bone diseases between Africa and other parts of the world meaning that relative Sr levels of subjects from all these regions are likely to be different.

Osteoporosis, which is the porosity of bones, has been found to affect some bones more severely than others. These bones include the spine/back, the hipbone, the wrist and the phalanges. All these bones are expected to have the same fracture risk when osteoporosis sets in since earlier studies reported that Sr and Ca were evenly distributed throughout the human skeleton (Nielsen, 2004). It is not clear why for example, an osteoporotic femur may break at the middle or at one of the ends or wherever. The clarity of this locational breakage will most likely depend on the elemental density across the bone.

Meunier et al. (2004) studied young menopausal women and osteoporosis. They reported that women were at a higher risk of experiencing the disorder as compared to their male counterparts. This shows that there could be a difference in Sr levels in human bones between male and female subjects, contrary to studies reporting constant relative Sr in human bones, among other factors such as weight of the bone and also the length of the bone.

1.3 Justification

Doublier et al. (2011) investigated the distribution and mineralization of Sr in iliac bone biopsies from osteoporotic women, treated with long term administration of Sr ranelate. They were able to demonstrate higher focal Sr in new bone structural units than the old ones during the treatment. Meunier et al. (2004) reported that Sr ranelate

reduced the risk of vertebral fractures in young menopausal women with severe osteoporosis. These studies did not provide information on the concentration and distribution of natural Sr in the human bone but highlighted the importance of Sr in the human bone.

Cesareo, Napolitano, and Iozzino (2010) studied the use of Sr ranelate as a treatment agent for metabolic bone disorders and observed Sr reduced vertebral and non-vertebral hip fractures over the 1st, 3rd, 4th and 5th years respectively. They concluded that its spectrum of activity would cover osteopenia and osteoporosis including its severe version. According to them, the safety profile of Sr as a drug compared to other anti-osteoporosis drugs was more positive. A nutrition study by Pagano, Yasuda, Roneker, Crenshaw, and Lei (2007) discovered that Supplemental Escherichia coli phytase and Sr enhance bone strength of young pigs fed on a phosphorus adequate diet. This further showed the growing importance of Sr as a bone mineral that was worth being investigated in Kenya.

In Kenya, information on the status of relative Sr in human bones at the inception of the main study was unavailable whilst metabolic bone disorders, such as osteoporosis, were prevalent in the country (Kamau, 2011). This motivated the main study which was expected to generate information that was going to improve our knowledge on the status of relative Sr in human bones in Kenya and possibly contribute in innovating methods of treatment and prevention of osteoporosis and other mineral bone disorders.

1.4 Scope and hypothesis

The study nondestructively analyzed femurs from human skeletons of a Kenyan population with the expectation that Sr, relative to Ca and Zn, was unevenly distributed across the human femur. This was because different regions of the femur were considered to have different architectural and structural designs and performed

different bone functions. Another reason for the hypothesis was the observation that bone elemental deposition was a random process that depended on different biological factors. It was also expected that there was a correlation between the relative Sr levels and the morphometric parameters of the femur (length and mass). This followed from the biological definition of the growth (an irreversible increase in the dry mass of an organism) and as such, massive or longer bones should ideally translate to more deposits of bone elements.

1.5 Objectives

To investigate relative Sr across the human femurs using bones obtained from the Department of Human Anatomy, University of Nairobi, Kenya.

The specific objectives were as follows:

i) To investigate the regional distribution of Sr to Ca ratio in the femur.
ii) To investigate correlation between the mass of the femur and average Sr to Ca ratio.
iii) To investigate correlation between the length of the femur and average Sr to Ca ratio.
iv) To investigate Sr to Zn ratio distribution and correlation to length and mass of the femurs.

Chapter 2

Literature review

2.1 Introduction

A number of studies have been done on bone mineral density of different human bones but information on the distribution of relative strontium within the human skeleton is not yet clear. Most of the studies have been done in Europe and Northern America and have used methods that are slightly different from conventional energy dispersive x-ray fluorescence technology which was used in this study. Other studies have assessed the bone mineral density in sections of other long bones such as the tibia and found it to depend on the age, region and gender. Some studies have analyzed the bone element depth distribution in the femur and found it to be fairly constant. To the best of the literature review and at the time of writing this thesis, there were no direct comparative studies in assessments of correlations between relative bone elements and bone morphometric parameters. As such, the discussions in the literature review have taken an indirect approach in some cases such as use of the body mass index when assessing effects of mass and/or length in variations of element densities across bones.

2.1 Regional distribution of relative strontium in long bones

Silverstein, Moeller, and Hutchinson (2011) define long bones as those that are hard, dense and provide the body with strength, mobility and structure. An electron microprobe analysis on excavated femurs was done by Lambert, Simpson, Buikstra, and Hanson (1983) to investigate their elemental distribution. The samples used were obtained from the Gibson and Ledders woodlands population in Florida, USA. These were cut into thin cross-sections for analysis using a scanning electron microscope. Sample preparation involved embedding the cross – sections in a methyl methacrylate polymer resin. Here, the sections were cut transversely using a high - speed diamond blade band- saw. These were then soaked in ethanol to remove their

surface debris and further cut into triangular wedges for identification of the inner and outer surfaces of the femur. The wedges were then mounted onto a carbon stub using tweezers and liquid graphite. The carbon stub was dried and mounted onto an aluminium stub in the SEM's vacuum chamber with epoxy. The nonconductivity of carbon resulted in the mount being carbon coated to a depth of approximately 300 Å in a JEOL model JEE 4C evaporator. Each element was then analyzed separately and a visual representation produced. In the visual representation, dots, whose density signified the relative concentration of elements involved, were used. The results for Sr showed that it was homogenously distributed throughout the femur compared to Fe, Al, K and Mn which had a buildup penetrating as from 10 to 400 µm into the bone. These results did not explain the frequent breakage of the proximal femur compared to the medial shaft and the distal femur.

George V Alexander, Nusbaum, and MacDonald (1956) investigated the relative retention of Sr and Ca in the bone tissue. The samples used included: femurs of Carworth strain mice, Wistar strain rats, albino guinea pigs, Nevada Kangaroo rats and rabbits, domestic rabbits, a horse and a cow. These were thermally ashed and then analyzed for Sr using emission spectrographic procedures. Ca in the laboratory animal femurs was determined using titration of precipitate oxalate with standardized permanganate. A flame photometer was used to analyze the Ca content of the desert animal samples. Bone ash, for Sr determination, was dissolved in a solution containing 1mg of CrO^3 and HCl to give a concentration of 30 g l^{-1}. A drop of the sample solution was then evaporated on a collodion treated 0.25 inch graphite electrode and then burnt in a 5A direct current arc after which the spectrum was photographed. The results showed that there was presence of Sr in all the animal bone samples while the Sr to Ca ratio among rat and mouse samples remained constant. It was also observed Sr to Ca ratio remained constant even for elevated Sr intake and that the number of atoms of Sr for1000 atoms of Ca present in bone samples ranged from 0.19 for rats to 2.5 for guinea pigs. Sr to 1000 Ca atoms ratio was found to be relatively constant for members of a given species regardless of their

age. This ratio was also found to be lower in bone compared to the diet. This generated interest in studying human femurs now that new information appeared to suggest Sr was a bone strength indicator.

Wada et al. (2001) investigated the relationship among the bone mineral distribution, static alignment of the knee and its adduction moment in patients suffering from tibio-femoral osteoarthritis. They used sixty nine patients who underwent radiographic evaluation, gait analysis and bone mineral density measurements at the proximal tibia and the lumber spine after a 4 week washout period of anti – inflammatory medications and physiotherapy. The proximal tibia were analyzed by a DXA system where antero-posterior measurements were made when the patient was in a supine position with the lower leg and knee in such a position as to ensure the tibia was parallel to the DXA table. A prosthetic hip sub-region mode was then used to scan the sections of interest. These scans were repeated three times in different days but within 28 days with repositioning between the scans for precision purposes. The variation of bone mineral density coefficients in the medial, lateral, anterior and posterior sections on the proximal femur were determined to be 4, 2-3 and 3 respectively. Results from this study summarily showed that the medial proximal tibia had a higher bone mineral density than the lateral compartment (at $P<0.05$ for mild osteoarthritis bones and $P<0.001$ for severe osteoarthritis cases). They also showed that the BMD was higher in the posterior region of the medial compartment than the anterior (at $P<0.05$ for mild osteoarthritis and $P<0.001$ for severe osteoarthritis cases). Bone mineral densities for the tibial regions analyzed were found to correlate with each other with correlation coefficients ranging between 0.43 and 0.77 ($P<0.01$). Findings in this study were attributed to the larger loads borne at the regions of higher BMDs. The study left interest in studying healthy femurs, other weight bearing bones, and the specific elements involved in their bone mineral matrices.

Sievänen, Oja, and Vuori (1992) studied bone mineral densities in different skeletal sites including the femoral neck and the distal femur. Fifteen volunteers, 3 male and 12 female, of mean age 38.1 years, mean height 167.5 cm and mean weight 68.5 kg were involved. The bone mineral densities and bone mineral contents were measured using a DEXA densitometer. In the analysis of the femoral neck, the subjects were positioned and images acquired using a scan with a pixel size of 1x1mm and a scan speed of 45mm/s. During the distal femur scan the subjects laid with their right sides after positioning their lower legs at 120^0 knee angles. This was achieved using appropriate supports. BMC and BMD measurements were repeated three times within a 2 week period. The coefficients of variation for both BMD and BMC were calculated resulting in a mean BMD (g/cm2) of 0.894 for the femoral neck against 1.291 for the distal femur and a mean BMC (g) of 4.73 and 40.8 respectively. These results showed that differences existed in the average mineral distribution across the femur but did not explain this observation. This study also failed to outline which particular minerals were varying across the femur and how.

Khodadadyan-Klostermann, von Seebach, Taylor, Duda, and Haas (2004) investigated the distribution of the bone mineral density across the proximal tibia among subjects that varied in age and gender. The samples, which included 40 human tibiae whose average age was 63.3 years with 27 being female, were selectively obtained from post-mortems, and frozen at -15^oC in readiness for analysis. The sampling process was biased so as to ensure that the selected bones were free from bone anomalies in all dimensions. Quantitative computed tomography and indentation testing was then used to obtain the bone mineral densities and forces to first failure values respectively. Results from this study showed that there was a statistically significant correlation between the maximum force to failure of the analyzed bone and its BMD ($\rho=0.822$ at $P<0.01$). The BMD of the proximal tibia decreased with age since it was higher in samples with an age of less than 60 years ($p<0.01$). Samples from males displayed a higher level of BMD throughout their volumes ($P<0.005$) compared to those from females. Additionally BMD was found

to consistently decrease from the proximal to the metaphyseal ($P<0.01$) with the lowest being observed at the antero-medial and central regions. In the male group of samples, the highest BMD was reported at the postero-medial, the antero-lateral and the postero-lateral regions. This study clearly shows regional differences in bone minerals in a long bone but neither investigated the rest of the tibia (and other long bones such as the femur) nor the variation of the specific minerals that constituted the stated BMD values.

Crabtree et al. (2000) researched the bone mineral distribution, hip geometry and bone strength in European men and women based on their proximal femurs. They used the lunar DPX "beta" versions of the hip strength analysis and hip axis length software to analyze radiographic scans of 10 representative samples from the European Prospective Osteoporosis Study which included 1617 patients of less than 50 years of age. The coefficient of variation for the bone mineral density of the upper half of the femoral neck was found to be lower than that of the lower half (2.6% versus 1.1%). The hip axis length is normally bent from the shaft but the femoral neck cross sectional moment of inertia showed no significant age reduction. These results suggested substantial differences in the BMD of the femoral necks accounting for the variations in the hip fracture risk across Europe. This study neither explained the specific mineral variation across the femoral neck nor causes for breakages below it.

Moffat et al. (2008) investigated the characterization of the structure – function relationship at the ligament to bone interface based on the BMD of the distal femur and the proximal tibia and their mechanical stresses. The mineral presence and distribution were characterized by the energy dispersive X – ray fluorescence analysis and backscattered electron microscopy. The samples were fixed in 100% ethyl alcohol for 24 hours then transversely cut to obtain different regions of the bone. These were then splutter coated with palladium and imaged by the backscattering SEM. In the energy dispersive X – ray analysis, points for irradiation

were randomly chosen per an interface region after which analysis was done at 20kV. Line scan analysis was then done to obtain elemental distribution across the interfaces. Bright images from the backscattering SEM scans corresponded to elements with large atomic numbers mainly calcium and phosphorus showing that bone regions of the proximal tibia and distal femur were made up of mineralized porous matrix. Results from the energy dispersive X – ray analysis showed that there was presence of calcium phosphate which varied regionally at the interface of the femoral and tibial insertion sites. It was also observed that the material properties of the analyzed samples strongly correlated with their mineral contents (R: 0.8835 for Young's modulus against the intensity of calcium and R: 0.8677 for the Young's modulus against the peak intensity of phosphorus). It was further shown that sulfur decreased from the interface to the bone regions while calcium and phosphorus increased. Conclusions from this study suggested that the femoral interface had less mineral density compared to the tibial interface because of the load transition. This could however not explain the frequent reported cases of osteoporotic fractures in bones with high bone mineral densities or the frequent breakages at the hip axis length of the proximal femur.

2.2 Correlation between the mass of the femurs and average relative Sr net intensities

Berger et al. (2010) researched the peak bone mass from longitudinal data and the implications on the diagnosis, prevalence and pathophysiology of osteoporosis. 615 women and 527 men with an age range of 16 to 40 years had their peak bone mass approximated using longitudinal data from the Canadian Multicenter Osteoporosis Study. Clinical assessments done included the height, weight and bone mineral density. In the BMD assessment, the lumbar spine, femoral neck, total hip, greater trochanter and Ward's triangle were analysed using DXA densitometers. These instruments were calibrated at the start of the study then annually using the bona fide spine phantom. Results from this study showed that BMD changes in younger

women were positive from 16 to 32 years of age but nil between 33 and 40 years. Peak bone mass of the average skeleton was therefore thought to have been achieved between the ages of 33 to 40 years. In the total hip and femoral neck, the BMD changes were nil between 16 and 24 years meaning that peak bone mass was achieved during this time or prior to 16 years of age. In the trochanter and Ward's triangle, a decrease in the BMD could be seen by 16 years of age showing that the peak bone mass had been achieved. Results for male subjects showed a similar trend. In a more specific but relevant approach, the lumbar spine peak bone mass (1.046±0.123 g/cm^2) was found to occur in women of ages 33 to 40 years and males of ages 19 to 21 years where it was observed to be 1.066±0.129 g/cm^2. The analysis of the total hip revealed a peak bone mass of 0.981±0.122 g/cm^2 for females of ages 16 to 19 years and 1.093±0.169 g/cm^2 for the sampled males in the age bracket 19 to 21 years. In summary, this study showed that the peak bone mass was dependent on the bone mineral density and the age of the subject but could not explain which specific minerals varied with the bone mass. This study also showed differences in peak bone mass across different skeletal sites alluding to a region dependent bone mineral deposition process whose specifics are addressed by the specific objectives in this thesis.

Cvijetić Avdagić et al. (2009) investigated the differences in the peak bone density between male and female students. They used 51 male and 75 female subjects whose heights and weights were measured after which DEXA scans were used to determine their areal bone mineral densities. The bones analyzed included the lumbar spine, the proximal femur and the distal third of the radius. Results from this study showed that men were taller (179.4±5.6 cm versus 167.5±5.8 cm at $p<0.0001$), heavier (78.4±7.1 kg versus 59.9±6.8 kg at $p<0.0001$) and had a greater body mass index compared to the females (24.4±2.2 kg/m^2 versus 21.3±1.9 kg/m^2; $p<0.01$). The bone mineral density, bone mineral content and bone area measured were found to be higher in boys than in girls for the spine, neck and distal radius (for example the spine BMD: 1.313±0.138 g/cm^2 versus 1.305±0.139 g/cm^{2,} BMC: 79.60±12.41 g versus

69.61±13.54 g, Area: 62.16±5.58 cm^2 versus 53.50±7.59 cm^2). BMD of the total femur in the female group was significantly predicted by both the body weight and dietary fiber at $p<0.0001$ and $p<0.01$ respectively. This study neither pointed out the exact minerals that made up the bone mineral density nor did it explain why heavier bones were also prone to fracture in osteoporotic patients.

2.3 Correlation between the length and average relative Sr net intensities

The overall height of a person has its basis on the length of their bones. The body mass index is the ratio of the mass to the square of the height meaning that the length of bones is a factor in the body mass index. Fawzy et al. (2011) studied the body mass index of patients referred for DEXA scans against their bone mineral densities. The patients had metabolic syndromes, bone diseases and few could not walk properly. These patients were subjected to femoral neck and lumbar spine scans for nine months using a DEXA densitometer following measurements of their heights and weights. Results from this study showed that BMD was significantly low in: 82.4% of the subjects with a normal body mass index, 78.1% of the overweight group and 44.2% among the subjects classified as obese. Further analysis showed that the obese subjects were less likely, by 89%, to develop low BMD compared to the rest. These results summarily suggest that lower BMI or larger bone length, by inference, compared to the overall subject's mass was a risk factor for low BMD (normal BMI was between 18.5 – 24.9 kg/m^2 while the obese had a BMI of over 30 kg/m^2). This study neither explained the reasons behind its findings nor did it outline the specific minerals that composed its BMD.

Alekel et al. (1999) studied the lifestyle and biologic contributors to the proximal femur bone mineral density and the hip axis length in groups of menopausal women. The subjects included Indian/ Pakistani and American Caucasian women between the ages 20 and 40 years with a body mass index between 16 and 30 kg/m^2. The proximal femur mineral measurements were done by the DXA and the Hologic bone

measurement software specifically at the trochanter, femoral neck and hip axis length. Results from this study showed that the height of the American Caucasian women was significantly larger than their Indian/ Pakistani counterparts. The bone mineral densities in gcm^{-2} were found to be lesser (0.875 vs 0.937 and 0.652 vs 0.705) for both the proximal femur and the trochanter in the Indian/ Pakistani subjects compared to their American counterparts. The mean hip axis length was found to be shorter for the Indian/Pakistani women at 10.54 cm compared to the American subjects who had 11.11cm. In summary, this study suggested that higher BMDs were associated with longer bones. It could however not explain the specific mineral re-adjustment and distribution that accounted for the increase in the BMD of the long bone. These results could also not explain why the prevalence rates for osteoporotic fractures were higher in the American population yet they had higher values of bone mineral density.

Another study on the hip axis lengths of the femur and their average bone mineral density was done by Goh, Low, and DasDe (2005) on Singapore's multiracial population. 1575 women, 1222 Chinese, 122 Malays and 231 Indians, aged between 20 and 59 years underwent bone mineral measurements including the determination of their hip axis lengths. Chinese and Malay women of between the ages 50 and 59 years were found to have significantly lower bone mineral densities at 6.6% and 8.2% respectively compared to the Indian women. Measurements of the hip axis lengths showed that the Chinese women had 9.87 cm compared to their Indian and Malay counterparts who had 9.69 cm and 9.67 cm respectively. To a certain extent, these findings suggested that longer hip axis lengths were associated with lower bone mineral densities, a clear contradiction to the study earlier reported in this thesis by Alekel et al. (1999). Clarifications were therefore required in addition to determination of the specific bone minerals that might vary with the length of a specific bone.

2.4 Energy Dispersive X-Ray Fluorescence EDXRF

This element analysis setup was preferred because it is fast, accurate, non–destructive and has a high precision and reproducibility of results compared to AAS–AES, PXRF and PSA. It could also analyze elements ranging from Na to U with concentrations of up to 100% (Markowicz & Van Grieken, 2002). An EDXRF system as shown on the setup in figure 1 uses x-ray radiation to produce fluorescent radiation from a sample which carries information (the fluorescent radiation) that can be used to determine the elements in the samples and their amounts.

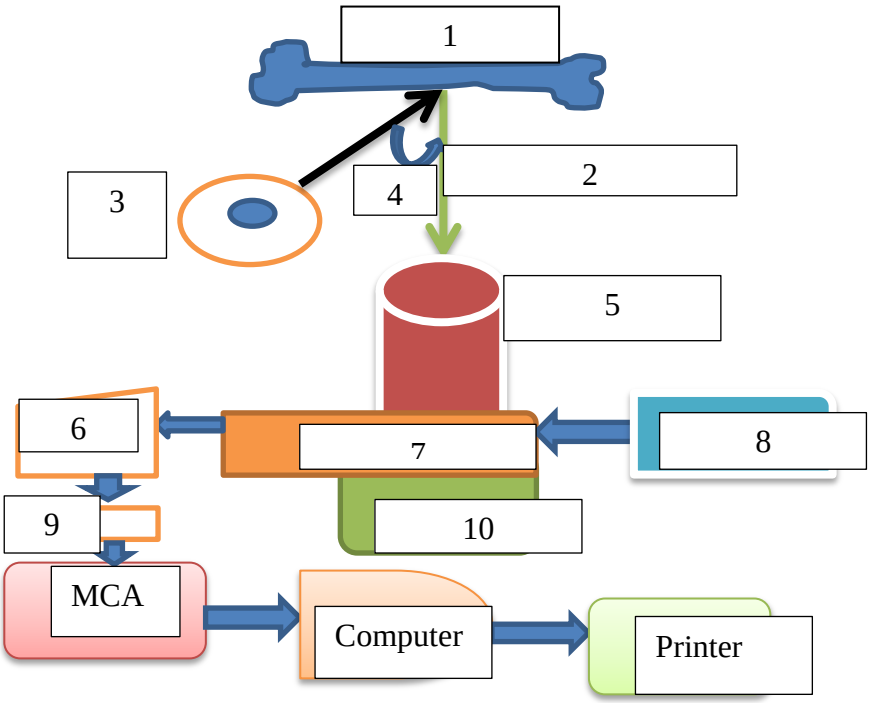

Figure 1: The EDXRF System components, ADC is Analogue to Digital Converter and MCA is Multi Channel Analyzer

Key

1: Human bone sample

2: Characteristic X-rays

3: ^{109}Cd source emitting Ag K X rays 22.2 to 25.5 keV

4: 46.6^{o}

5: Si(Li) Detector

6: Amplifier

7: Pre – amplifier

8: Detector Bia

9: ADC

10: Liquid Nitrogen

The x-rays are produced by ^{109}Cd, which has a half-life of 1.26 years and decays through electron capture resulting in excited ^{109}Ag which de-excites by emission of gamma rays of energy 88 keV in 3.6% of the de-excitations and K x-rays of energies 22.2 to 25.5 keV in the remainder of the de-excitations (96.4%). The following is the decay process equation for the primary x-rays used:

$$^{109}\mathbf{Cd} + \mathbf{e} \rightarrow \quad ^{109}\mathbf{Ag} + \mathbf{x\text{-}rays\ (22.2\ to\ 25.5\ keV)} \qquad \mathbf{(i)}$$

The primary x – rays can possess sufficient energy to ionize atoms of a sample being analyzed by dislodging electrons from specific shells thereby leaving the atoms in an unstable state. These atoms regain stability by undergoing an internal reorganization of their electronic configuration where electrons from higher orbitals move to occupy vacancies left behind by the electrons which were dislodged by incident primary radiation. This results in emission of characteristic fluorescent radiation which is unique to different elements and whose energy is the difference in the energies of the orbits that were involved in electron transition. The intensity of the fluorescent radiation is directly proportional to the quantity of the element that it represents. The system's detector is capable of detecting different energies of characteristic radiation coming directly from the sample; a process called dispersion. Scattered radiation from the source accounts for the background noise in the spectra. The detector is constructed from a semiconductor material (silicon) and has a beryllium window that allows X–ray photons to access the detector (Figure 2).

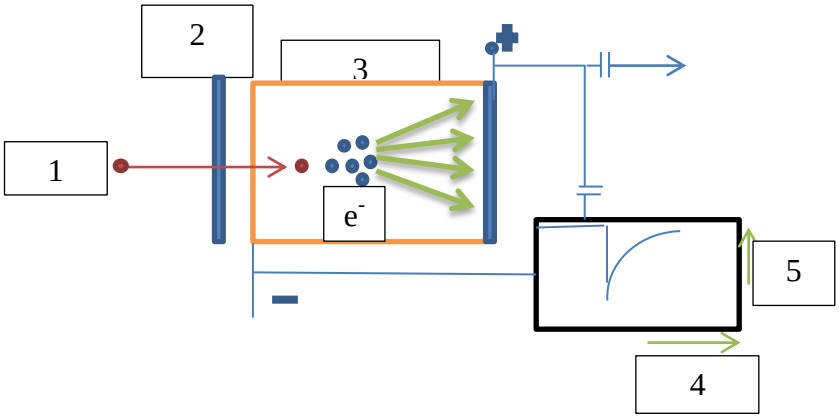

Figure 2: The Lithium drifted Silicon radiation detector diagram

Key

1: Photon

2: Be window

3: Detector Body

4: Time

5: Voltage

The detector sensitive diameter was about 1.01 cm which was suitably less than the average femur matter to be placed on the sample holder by values ranging from approximately 0.5 cm to about 3 cm, depending on the cross sectional length of a specific irradiation partition within the femur. This would ensure that the fluorescent radiation from the bones is largely incident on the detector. Irregularly surfaced samples did not have a major impact on the intensity of the fluorescent radiation as x–rays were almost un – attenuated, at 0.99995 of the original intensity, for less than 5 mm of moderately clean dry air near sea level. This was deduced based on estimates involving the Beer – Lambert law, (Saloman, Hubbell, & Scofield, 1988).

Consider:

$$\frac{I}{I_o} = e^{-\frac{\mu}{\rho}\rho x} \qquad \textbf{(ii)}$$

Where:

I – Emergent intensity from the dry air volume.

I_o – Incident intensity on the dry air volume.

$\frac{\mu}{\rho}$ - Mass attenuation coefficient for 20 keV X rays in dry air (0.778 $cm^2 g^{-1}$).

ρ – Density of dry air ($1.21 \times 10^{-3} g cm^{-3}$).

x – Estimated X ray path length in air (0.5cm).

Fluorescent radiation enters the detector volume and creates electron hole pairs, which are swept by a bias voltage thereby generating a current that is observed as a pulse. The pulse height is proportional to the number of electron hole pairs and the incident radiation energy. The detector thus converts secondary fluorescent radiation into electrical signals, which are amplified and presented to the analogue to digital converter, ADC. The ADC converts the analog signal to a digital signal represented by a number of clock pulses, which address memory locations in a Multi-Channel Analyzer (MCA). The MCA creates and shapes a representative histogram/spectrum (appendix A), which is stored, displayed, analyzed and retrieved using a computer.

Chapter 3

Materials and Methods

3.1 Sources of Material

This research involved samples of human bones, which were collected from the Department of Human Anatomy at the University of Nairobi (UoN) and taken for EDXRF analysis at the Institute of Nuclear Science and Technology (INST).

3.2 Sample Selection Criteria

Human bones were selected according to the specific objectives and availability of the required sample quantity. The sampling process aimed for an optimum sample size that would provide statistically meaningful results. The femurs are major weight transmission bones and as such they were selected for investigation. After the femurs the humerus, ulna, tibia and radius were to be analyzed. The sample size was determined in accordance with recommendations by Dell, Holleran, and Ramakrishnan (2002) and to begin with, sixteen femurs were randomly selected as they were the maximum that would fit into the selected carton for efficient transportation.

3.3 Sample Preparation

Prior to being transported to INST laboratory, the samples had been boiled, macerated off the human tissues, dried and stored in a clean and moist free containment at the Human Anatomy laboratories. Selected femurs were taken to the Department of Civil and Structural Engineering laboratory, University of Nairobi, for morphometric measurements, which included determination of lengths and masses using a tape measure and a weighing balance respectively. The lengths of the femurs were measured from their heads to the medial condyles using a tape measure whose

sensitivity was 0.1 cm. The masses were measured by placing the bones, one at a time on a top pan electronic balance with a sensitivity of 0.01 grams. At the INST lab, the bones were further cleaned using double-distilled water to remove any foreign materials such as dust from their surfaces. They were then dried and labeled, using a masking tape, at nine selected points, which were about 5.7 cm from each other along the shaft (Figure 3). This was the case as 5.7 cm was the approximate diameter of the primary radiation source housing (figure 4) and as such the partitions would be well isolated from one another. The other irradiation partitions included prominent regions of the femurs as follows: Point b1 was the medial condyle, b2: lateral condyle b8: greater trochanter and b9: head of the femur.

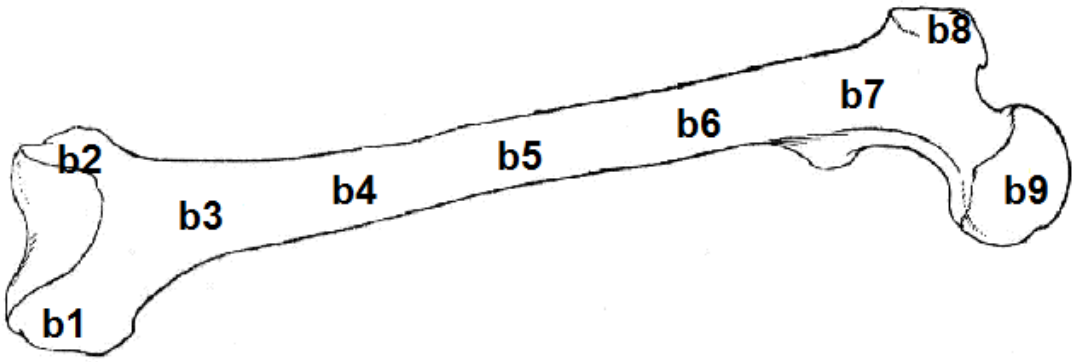

Figure 3: Human femur showing the selected irradiation partitions

3.4 Instrumentation

An EDXRF system, as partly described in section 2.4 of the literature review, was used to analyse the prepared samples for information on the net intensities of relative Sr across the sample surfaces. The system included a make shift sample holder, primary radiation source, detector with associated electronics and a computer as in figures 1 and 4. The femur was held in irradiation position by a system of plastic, paper and rubber structures such that the flattest part of the irradiation point rested on the center top of the primary radiation source which produced X rays from the electron capture of ^{109}Cd. Every selected partition was then irradiated for 1800

seconds since longer measurement times were expected to increase the precision; reproducibility of results and reduce uncertainties. Longer irradiation times were also expected to reduce the detection limits of the EDXRF system but would have decreased the sample throughput hence the tradeoff time (1800s) used in this study. Characteristic fluorescent radiation was detected using the Si(Li) detector and converted into a representative histogram with the aid of electronic systems, within the EDXRF system, which included: the preamplifier, detector bias, amplifier, ADC, MCA and a computer.

3.5 Measurement setup

The setup is shown in a block diagram (Figure 1) and included a fabricated sample support as in figure 4. The figures (1 & 4) show the radiation source (^{109}Cd), detector (Si(Li)) and a personal computer among other components.

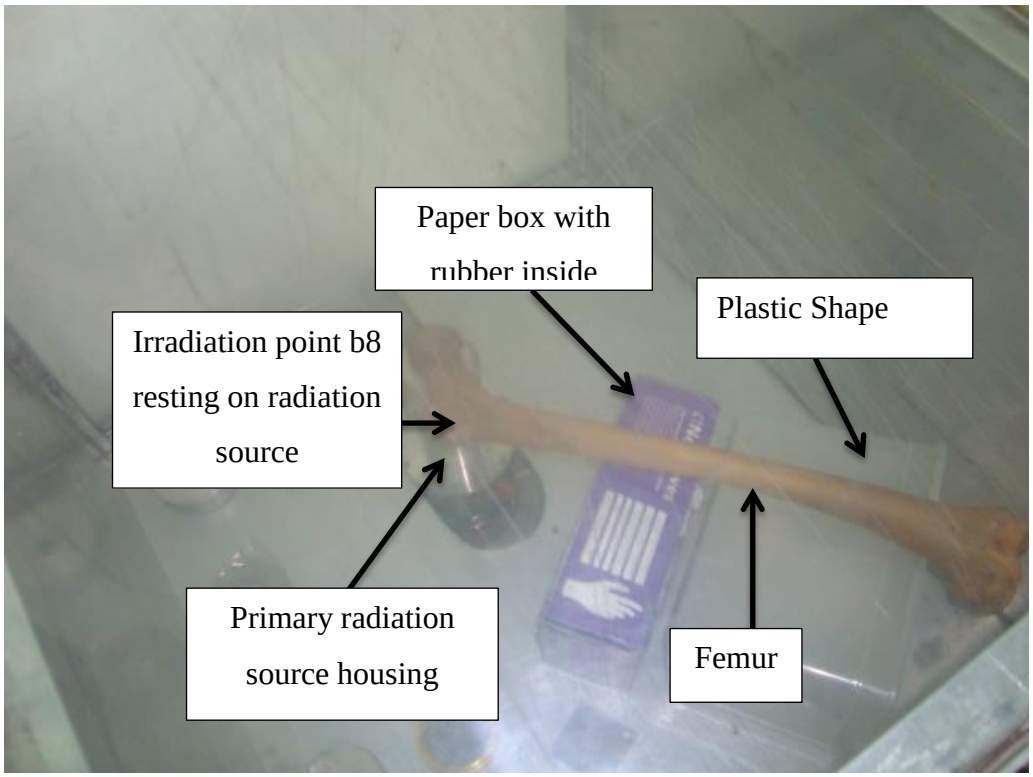

Figure 4: Sample positioning set up for irradiation

3.6 Spectra and Data analysis including Statistical treatment

The Spectra obtained from the MCA (figure 17 in the appendix section), , were transformed to net elemental intensities using the AXIL software as explained in section 2.4 of the literature review. These intensities were then normalized after which statistical techniques were applied to analyse the data further. In analysis of the regional distribution of relative Sr across the femur, averages and standard deviations of normalized relative Sr ratios, from similar irradiation partitions from the sixteen femurs, were calculated to enable comparisons through graphs and tables. These averages were further divided by average normalized net intensities for each femur meaning that b1, from F1 for example, was divided by the average intensity for F1. This was done so as to minimize the standard deviations which had initially appeared large. Bivariate correlation analysis was done to check if the element ratios of paired irradiation partitions differed significantly from each other. This was necessary so as to establish whether the relative Sr distribution was homogenous or heterogeneous. Correlations involving relative Sr and the mass or length of the femurs were analyzed through determination of the average relative Sr ratios from the nine irradiation points across each bone. Regression analyses were then used to determine whether there were significant correlations between the averaged ratios and the mass or length of the femurs. These analyses involved correlation coefficients R, percentage variability of the dependent variable linked to changes in the independent variable (R squared), ANOVA and t tests with their significance. The SPSS statistics software was used to graph and analyze all results of this study.

Guénin et al. (2009) writes that the quantity of a an element, molecule or compound in a biological sample depends on the size of the sample and therefore normalization would be important so as to account for the variations in measured quantities before comparing them. Gullion, Devous Sr, and Rush (1996) explain that normalization involves performing arithmetic transformations on data sets that contain individual differences so that it becomes common for comparisons to be done. In the main study

irradiation results reveal that the femur had three main elements based on the net intensities. These elements differed in terms on their molecular masses hence the need to normalize the net intensities based on the same.

Raw net intensities were therefore normalized as below:

$$\boldsymbol{N_R = \frac{I_N(Counts\ s^{-1})}{M_E(gmol^{-1})}} \qquad \textbf{(iii)}$$

Where:

N_R – Normalized result

I_N – Raw elemental net intensity

M_E – Molar mass of the element

M_E values were as follows: 87.62 $gmol^{-1}$ for Sr, 40.078$gmol^{-1}$ for Ca and 65.37$gmol^{-1}$ for Zn.

Ratios obtained are therefore based on normalized results.

Chapter 4
Results and Discussions

The results are displayed according to the specific objectives in graphical form and in tables that contain data from individual femurs. Tables used for the graphs and those representing bivariate correlations are in the appendix section. The study had hoped to irradiate a representative sample of bones for the entire human skeleton but the EDXRF system broke down after the irradiation of the first batch of the femurs which were 16 in number. This therefore meant that there were 144 results to be analysed as each femur had been irradiated at nine different partitions. This has been discussed as a limitation in section 5.3.

4.1 Average Sr to Ca ratios across the 16 femurs. b1 to b9 are the partitions along the bone as shown in Figure 5

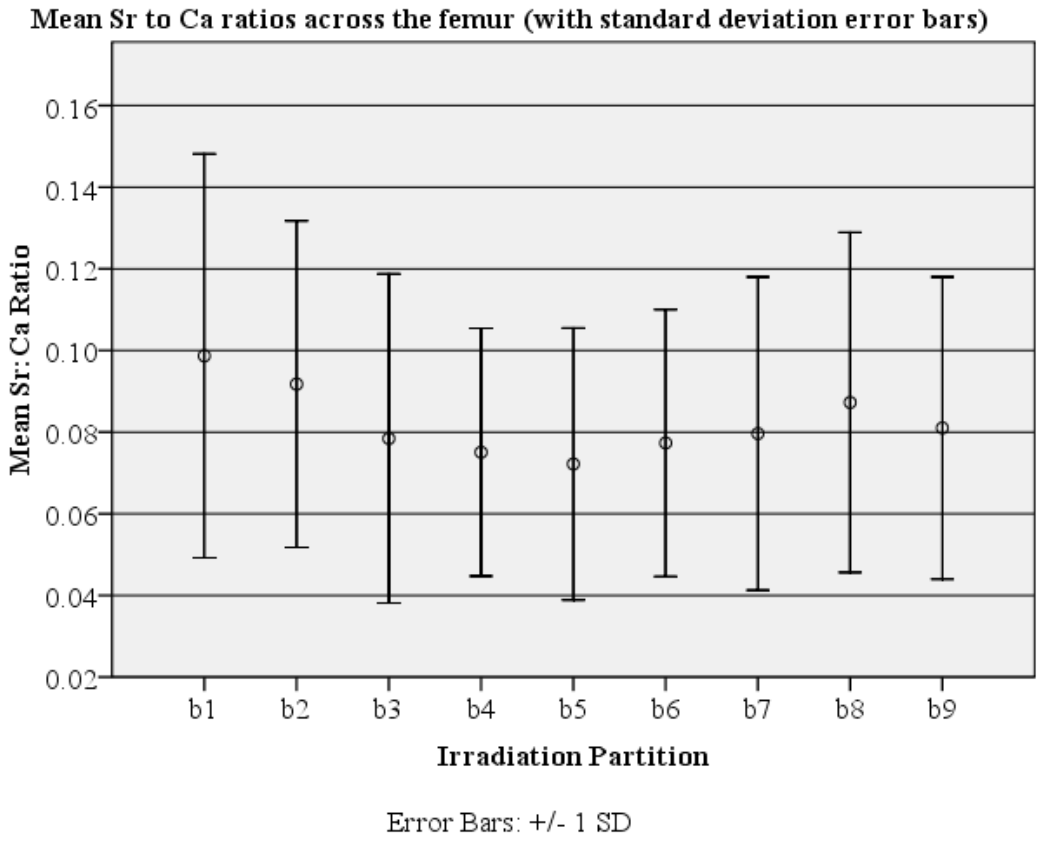

Figure 5: Average Sr to Ca ratios across the femur

Key

SD – Standard Deviation

The graph in figure 5 has been developed from processed data as in table 4 and it shows some variations in average normalized net intensities across the femur which are somewhat overshadowed by the considerable standard deviations. The large standard deviations might have arisen from person to person or femur to femur differences which were unknown other than the morphometric parameters and the fact that all the irradiated femurs were healthy. This showed the need for further

processing to minimize the standard deviations as explained in section 3.6 of this thesis.

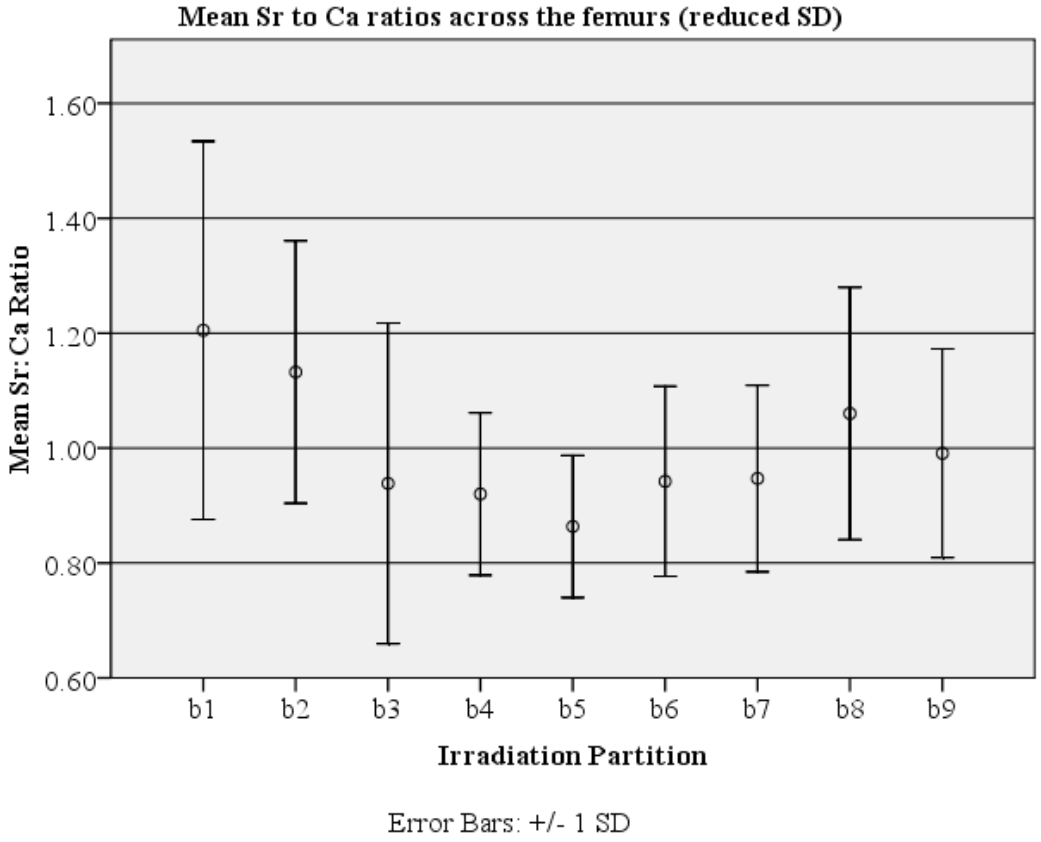

Figure 6: Average Sr:Ca ratio across the femur with reduced standard deviations

The graph in figure 6 has been developed from table 5 and shows that irradiation points b3 to b7 (shaft of the femur) and b9 (rounded head of the femur), which are made up of compact bone, had comparatively low (<0.085) normalized Sr to Ca ratios at 0.078, 0.075, 0.072, 0.077, 0.080 and 0.081 respectively compared to the other regions (>0.085) which mostly contained spongy bone. The graph also shows that points b1 and b2, which consist of the condyles, had the highest Sr to Ca ratio (>0.09) at 0.099 and 0.092 respectively. Point b8, the greater trochanter region, had

the third highest Sr to Ca ratio, at 0.087. The mid shaft, which is made up of the compact bone had the lowest Sr to Ca ratio at 0.072.

Table 1: Normalized Sr to Ca ratios (factors of 100 that have been rounded off to the nearest whole number) from randomly chosen femurs: F1, F7 and F15 – This has been obtained from table 4 in the appendices section

	b1	b2	b3	b4	b5	b6	b7	b8	b9
F1	15	10	8	7	8	7	7	7	7
F7	7	5	3	3	2	2	2	6	5
F15	8	8	6	7	7	5	6	7	6

Randomly selected femurs (F1, F7 and F15) showed slightly higher Sr to Ca ratios (Table 1) at the condyles (b1 and b2) compared to the other points which were relatively similar except for femur F7 which had the lowest Sr to Ca ratios across its shaft. These results show that variations of normalized Sr to Ca ratios depend on the architecture and position of the irradiation point. The compact femur bone has been described as being responsible for formation of a dense cylinder down the shaft, which surrounds the bone marrow cavity, (University of Cambridge, 2014). It is less porous and accounts for about 80% of the bone mass, see Figure 7.

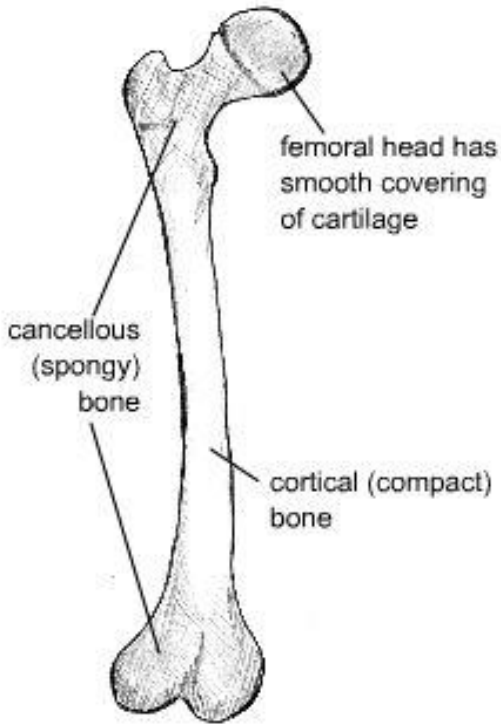

Figure 7: Anatomy of the femur (University of Cambridge, 2014)

The spongy or cancellous bone is found on the ends of the femur (except for the rounded femoral head); contains the rest of the femur mass and has a lower young's modulus compared to the cortical bone. Irradiation points with low Sr to Ca ratios have higher comparative Ca whose required amount in the bone is influenced by the bone region's architecture and geometry (Flynn, 2003). As reported in the literature review, Ca is the predominant element in the bone and this is reflected by findings in the main study which show that the compact bone had the highest Ca compared to Sr. These findings are similar to a study by Aitken (1976), which used atomic absorption spectrophotometry in analysis, to report higher relative Ca in the cortical or compact regions of the femur.

Bivariate correlations, in table 6 of the appendix, show that the distribution of Sr to Ca ratio across the sixteen femurs was relatively homogenous as there were only three femur regions that differed significantly in terms of their Sr to Ca ratio: b1 and

b3. This is seen by the fact that there was a correlation of 0.5 when comparing the two irradiation partitions with each other. All other paired irradiation points had significant correlations that were closer to 1 (red and blue at 0.01 and 0.05 levels respectively) meaning that they were reasonably homogenous. According to Dahl et al. (2001) Sr and Ca substitute each other in bones depending on a variety of ossification processes and this might explain the significant difference in Sr to Ca ratios between points b1 and b3 as well as the fact that b1 is in the condyle region while b3 makes part of the femur shaft. G.V. Alexander and Nusbaum (1959) studied the relative retention of Sr in the femurs of specific domestic animals using emission spectroscopy and flame photometry. They found out that the ratio of Sr to 1000 Ca atoms was relatively constant. These findings suggested that the average Sr to Ca elemental density across the femurs was relatively homogenous which was also reflected in an electron microprobe analysis by Lambert et al. (1983) where Sr levels in excavated femur cross sections were found to be homogenous. A study on quantification of Sr levels in bone by Pejovic et al. (2004) measured the Sr levels at particular sites in the human finger and the tibia. The results showed ratios of 0.23+0.81 mg of Sr to a gram of Ca for the finger and 0.34+0.65 mg of Sr to a gram of Ca for the tibia which also transits weight as the femur does. This difference was however found to be statistically insignificant. This study therefore further showed the constancy of the Sr to Ca ratio in two different bones.

4.2 Average Sr to Ca ratios and mass of the femurs (N=16)

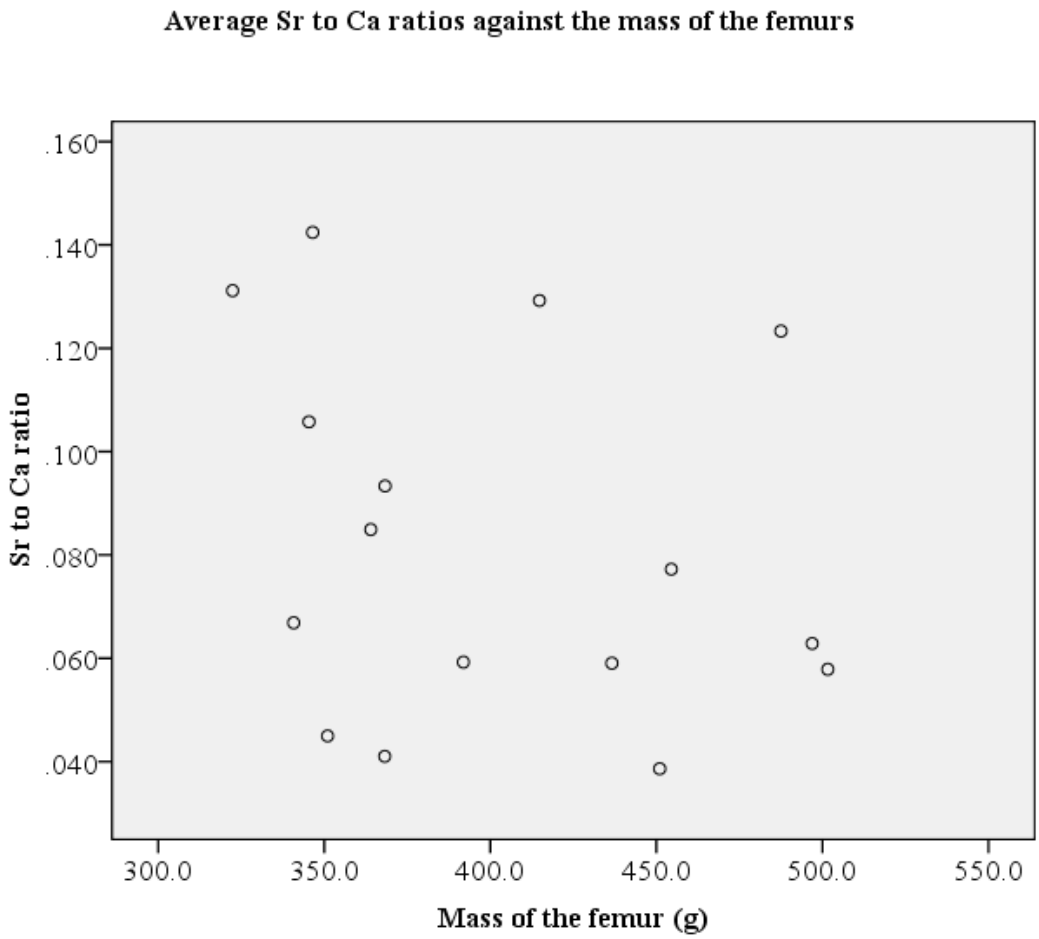

Figure 8: Average Sr to Ca ratios versus the mass of the femurs

The graph has been plotted from averaged normalized net intensities from each femur and their masses (table 4 and 10). These results (as in the graph) showed a correlation coefficient, R, of 0.252 with only 6.3% (R square value) of the total variation in Sr to Ca ratios being linked to the changes in the mass of the femurs (table 7 of the appendix). ANOVA showed an F test value of 0.947 with a significance of 0.347 that was more than the statistically accepted value of 0.05 or less for a linear relationship between the two variables. The standardized correlation coefficient was -0.252 with a t test value of -0.973 that was also insignificant at

0.347. All these pointed to an insignificant correlation between Sr to Ca ratios and the mass of the femurs. To the best of the literature review, there were no direct comparative studies in this area. These findings imply that Sr to Ca ratios across the femur do not depend on the mass of the femurs. A study by Felson, Zhang, Hannan, and Anderson (1993) revealed that the effect of weight on bone mineral density was in general much less in men compared to women and so this might explain the insignificant correlation if the bones used in the main study belonged to a mostly male population. The lack of gender bias in the irradiated femurs has been mentioned as a limitation in this study. Another study by Aitken (1976) suggested that it was the skeletal Zn content based on age that was related to alterations in bone morphology and not the Sr content (based on net intensities). This appears to be the reason why there is a correlation between the mass of the femurs and normalized Zn rather than relative Sr (figure 20 in the appendix) although the age factor could not be accounted for as the femurs were from an adult population whose specific age was unknown, this is also mentioned as a limitation in this study. This implies that heavier bones are not necessarily strong and may fracture in the event that the weight carried is in excess or if the bone is made to undergo a strenuous activity. Studies by Alekel et al. (1999) on Indian/ Pakistani Women in comparison with their American Caucasian counterparts found that femoral bone mineral density depended on age, lifetime non-pregnant weight and the composition of the bone matrix. They also discovered that the current weight of the subjects studied had no bearing on the femoral bone mineral density. This meant it was possible to have a weighty bone yet lower relative Sr when studying a point within the surface of the bone meaning that the bone was heavy but porous, with regards to relative Sr. The explanation for variance with lifetime non pregnant weight was given by Lanyon (1992) who expressed that an estrogenic stimulus comes about in the event of a mechanical strain following the bearing of a sufficient load that leads to an increase in bone mineral density. This observation was for bone mineral density and not necessarily relative Sr.

Overall, these results confirm the independence of bone strength on the mass of the bones since fracture incidences have been observed in both heavier and lighter bones. Factors that have been attributed to bone fracture, as earlier reported in this study, are the advent of bone mineral disorders such as osteoporosis and the mechanical stress experienced by the bone. This study has shown that there are higher relative Sr deposits at the condyle regions of the femur and higher relative Ca at the compact regions; it is therefore recommended that this be used to assess bone mineral densities. At the time of writing this thesis there were no clear or direct studies on the mechanical strength of bones against their morphometric parameters and therefore investigating this for Kenyan bones might explain further whether femur fractures are affected by the their overall mass.

4.3 Average Sr to Ca ratio against the length of the femurs

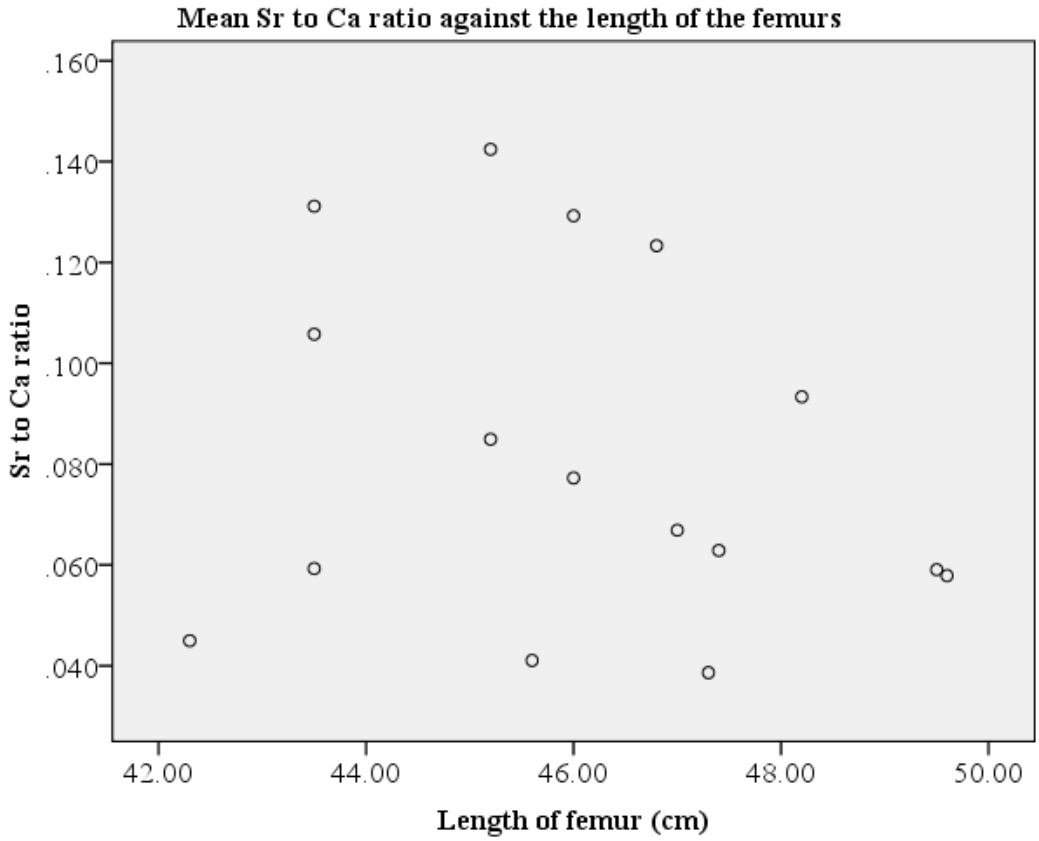

Figure 9: Average Sr to Ca ratios versus the length of the femurs

The range of the length of the femurs (between shortest and longest) was 7.3 cm, meaning that the largest irradiation partition would differ from the smallest by only 0.8 cm. This deviation was small enough to justify putting all focus on subdividing the femur to 9 irradiation partitions, that would be relatively equal along the shaft, rather than adding more irradiation sites. Regression analysis from the results in figure 9 showed the following: R value of 0.207, R square: 4.3%, F test statistic: 0.628 at a significance of 0.441, standardized correlation coefficient: -0.207 with a t test value of -0.792 and a significance of 0.441. These pointed to an insignificant correlation between average Sr to Ca ratios and the length of the femurs. At the time of writing this thesis there were no direct comparative studies in this area. These

findings imply that normalized Sr to Ca ratios do not depend on the length of the femurs and that longer or shorter bones may fracture based on other factors such as weight exerted, bone structure and other elements that make up the bone matrix such as Zn (figure 21). A study in Singapore by Goh et al. (2005) investigated hip fractures among the Chinese, Indians and Malay women. Findings showed that the Chinese women had the highest incidences of fracture and this was attributed to their measured hip axis lengths, which were significantly longer than the rest. Similar studies by Reza, Rahman, Hossain, and Afroz (2008); (Theobald et al., 1998; Turner, Liu, Manatunga, Timmerman, & Johnston Jr, 1995) showed that the longer the hip axis length of a femur is, the higher the fracture incidence. These studies attribute their findings to increased mechanical stress on longer bones as according to Serway and Vuille (2015) longer bones would increase the turning effect of a force applied at one end if the pivot was along the mid shaft. The force here is the actual weight exerted on the bone and hence this may increase the fracture incidence of this bone.

Another study by Alekel et al. (1999) investigated Indian/Pakistani women's femoral and trochanter bone mineral densities, using DXA, and compared them to their American counterparts against their fracture incidences. Findings showed that Indian or Pakistani women had low ($p=0.0014$) bone mineral density at 0.875 ± 0.096 vs 0.937 ± 0.088 (g/cm^2) for the total proximal femur compared to the American Caucasian women. The femoral neck bone mineral densities for the two groups were however statistically similar, ($p=0.054$) at 0.792 ± 0.093 for the Indian/ Pakistani and 0.828 ± 0.090 for the American Caucasian Women. When the hip axis lengths for these two groups were compared, the Indian/Pakistani women had 10.54 ± 0.57 cm while the American Caucasians had 11.11 ± 0.78 cm. The Hologic software was used to predict that the average hip axis length of the American Caucasians would have a 2.3 fold greater risk of fracture, based on its length, compared to their Indian or Pakistani counterparts. Regression analyses for these data however, showed that the femur length did not have a variance on the femoral bone mineral density, which, as reported earlier, is affected by age and lifetime none pregnant weight of the subjects that were studied. In summary discussions by Alekel et al. (1999) outlined that

although the Indian/ Pakistani women had shorter hip axis lengths, their low femoral bone mineral densities and other factors, such as lower serum $25(OH)D_3$ concentration and higher urinary N-telopeptide, would increase their incidences of osteoporotic fractures.

4.4 Sr to Zn distribution and correlation with mass and length of the femurs

4.4.1 Average Sr to Zn across the 16 femurs

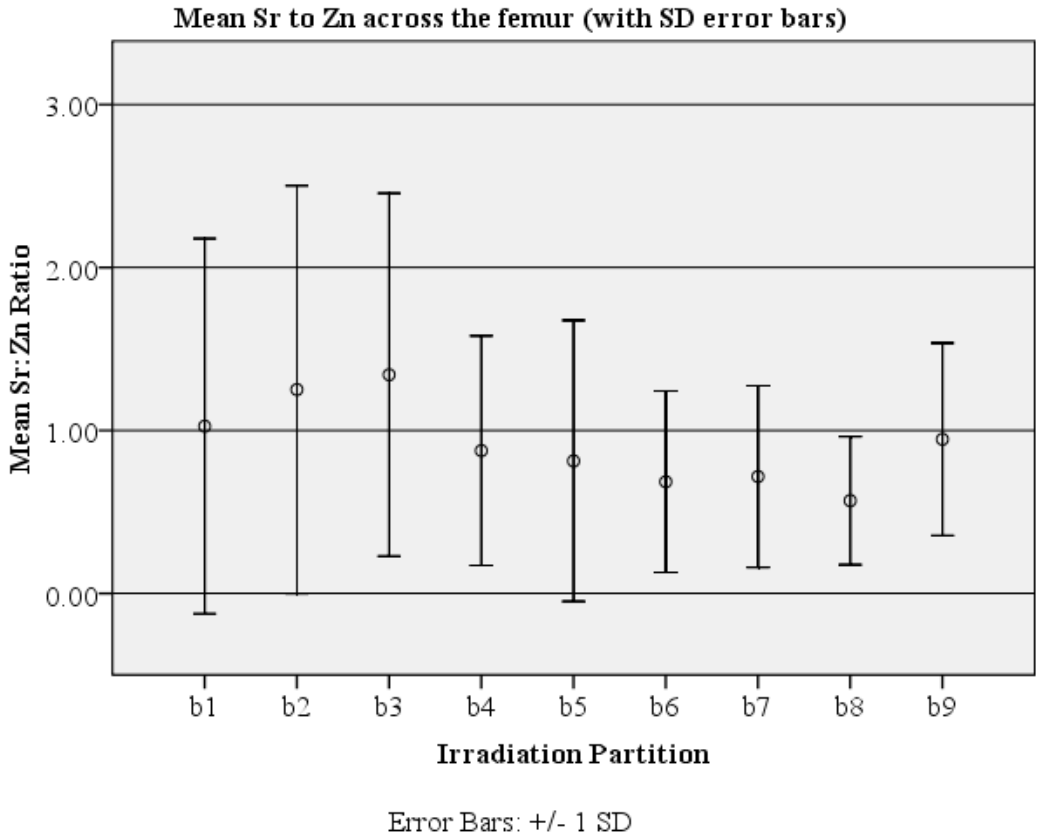

Figure 10: Average Sr to Zn ratio across the femur

The graph in figure 10 has been plotted from the inverse of Zn:Sr values in table 4 and includes error bars from standard deviations worked out per an irradiation partition for the sixteen femurs. Analytical procedures discussed in section 3.6 of this

thesis were applied to minimize the standard deviations so as to enable a fair assessment of the distribution of average Sr to Zn across the femur thereby resulting in figure 11.

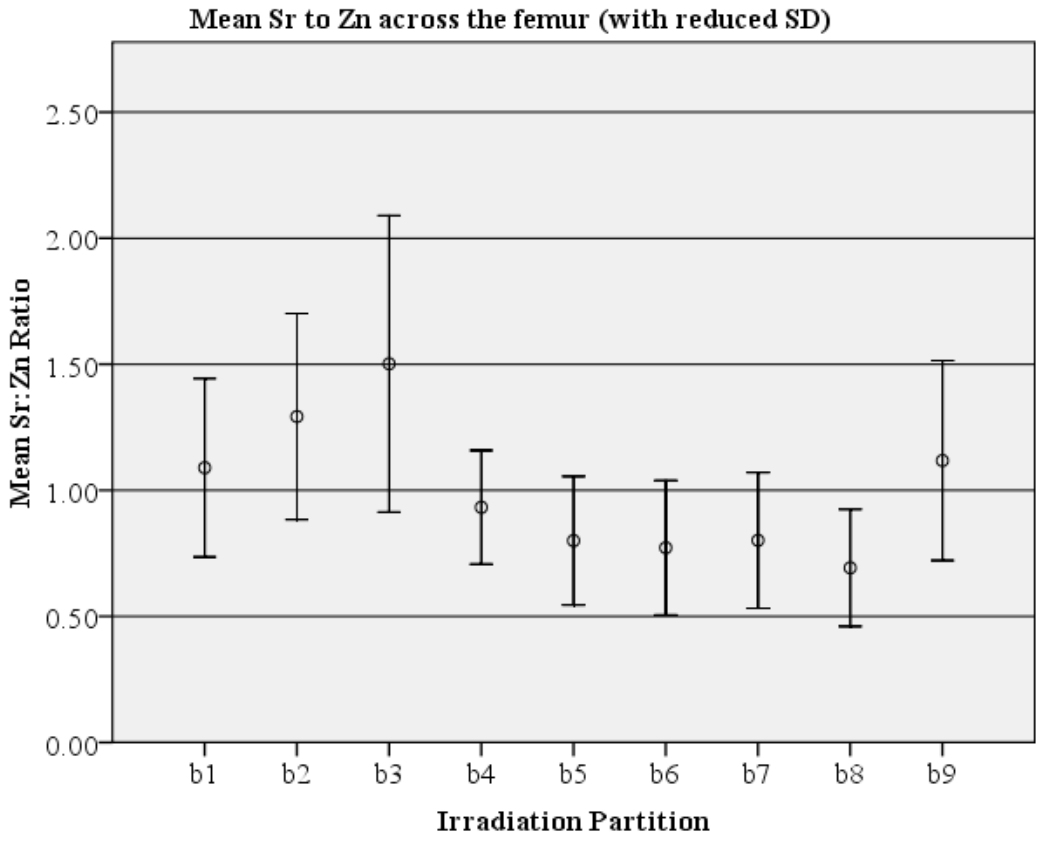

Figure 11: Average Sr:Ca ratio across the femur with reduced standard deviation

The graph shows highest normalized Sr to Zn ratios (>1.00) were observed at points b1 to b3 (1.03, 1.25 and 1.34 respectively) which included the condyles (b1 and b2) and the succeeding compact bone (b3). The shaft, which is mainly made up of the compact bone showed decreasing Sr to Zn ratios from the condyle region to the head region except from b6 to b7. The trochanter region, b8, showed the lowest normalized Sr to Zn ratio (0.569), compared to other points. The head of the femur had a higher normalized Sr to Zn ratio, at 0.946, compared to the trochanter.

Table 2: Normalized Sr to Zn ratios (rounded off factors of 10) for randomly selected femurs: F1, F7 and F15

Sr:Zn	b1	b2	b3	b4	b5	b6	b7	b8	b9
F1	6	8	11	3	2	3	3	6	9
F7	2	3	4	2	2	1	1	2	2
F15	13	16	8	9	10	6	16	9	12

In Table 2, femur F1 and F7 had the lowest normalized Sr to Zn ratios at their shafts (b4 – b7). In femur F15, the lowest normalized Sr to Zn ratio was observed at irradiation point b6. Sr has been linked with bone strength while Zn, as reported earlier in this thesis, is associated with stimulation of bone growth. A review of studies by Molokwu and Li (2006) shows that Zn is needed to maintain bone mineral density and bone metabolism leading to prevention and/ or reversal of osteoporosis. This might be the reason why there is an abundance of Zn or Sr at the cancellous femur which is by default more porous than the cortical bone. A study by Alekel et al. (1999) on lifestyle and biological contributors of the proximal femur mineral density using DXA found out that the trochanter had lower bone mineral densities at 0.652 ± 0.082 gcm^{-2} for Indian/ Pakistani subjects and 0.705 ± 0.073 gcm^{-2} for their American Caucasian counterparts compared to both the femoral neck and the total proximal femur which had 0.792 ± 0.093 gcm^{-2} vs 0.828 ± 0.090 gcm^{-2} and 0.875 ± 0.096 gcm^{-2} versus 0.937 ± 0.088 gcm^{-2} respectively. This could have been the reason why there were higher incidences of fracture at hip axis lengths of the femur, as reported in this study.

Studies on physical stress distribution on the femur through mechanical 2D modeling by Rudman, Aspden, and Meakin (2006) suggest that the opposite side of the trochanter is twice as strong in compression compared to the tensile side (b8: greater

trochanter). This observation might have been due to an osteo-adjustment of the bone to counter the increased compressional forces that come with the slight bending of the femur at the trochanter region. The tensile weakness of the greater trochanter can therefore be attributed to lower Ca deposits as observed in the main study and hence the need for the bone to compensate by having more Zn at the point. Another study by J. Y. Reginster et al. (2005) showed that a Sr compound, strontium ranelate, reduced the risk of vertebral fracture by 35% over 4 years of treatment of menopausal osteoporotic women. In this case, bone mineral densities increased by 15.8% in the baseline of the lumbar vertebrae and 7.1% in the femoral neck. Previous studies reported in this thesis show that relative Sr is a bone strength indicator and therefore regions that exhibit higher relative Sr can be considered to be stronger than the rest. The condyle region can therefore be considered to be stronger than the head region as it was observed to be possess more relative Sr and this might be explained by the fact that when a human being is standing, more weight is exerted at the condyle region of the femur and hence the necessity for this region to be much stronger compared to the others.

Another probable reason for the increase in Sr to Zn ratios at the condyles is the fact that this region contains cancellous bone which, according to Education Portal (2015), provides structural stability and houses most of the red bone marrow that is responsible for production of blood cells. Porosity at this region is therefore necessary and hence the need to strengthen it using relative Sr as Ca parse would make the region strong but then lead to compactness (Ca has a smaller molar mass compared to both Zn and Sr) which is not desired at this point. Basic physics desires that the regions of a structure that are expected to bear the highest weight be stronger and able to withstand higher stresses and strains compared to the rest. This explains why femur condyles have more Sr to Zn ratios. Studies by Alekel et al. (1999); (Fullerton & Snowdy, 1988; Goh et al., 2005; Plancher & Donshik, 1997) report high incidences of femoral neck axis/ hip length axis fractures compared to the other parts of the femur.

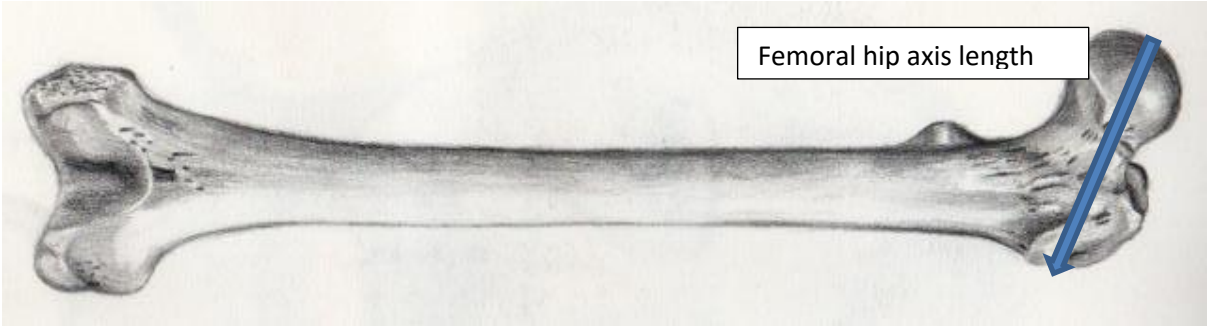

Figure 12: Femoral hip axis length

This may be due the findings that there is less Sr to Zn ratio in the femoral neck region of the femur compared to the condyle region although Zn also assists in bone growth. The implication here is that the femoral neck region is weak due to the reduced Sr to Zn ratios leading to higher incidences of fracture. Some studies, as reported in previous paragraphs in this section, show that the femoral neck has lower bone mineral densities and may easily fracture due to the same.

4.4.2 Average Sr to Zn ratios and the mass of the femurs

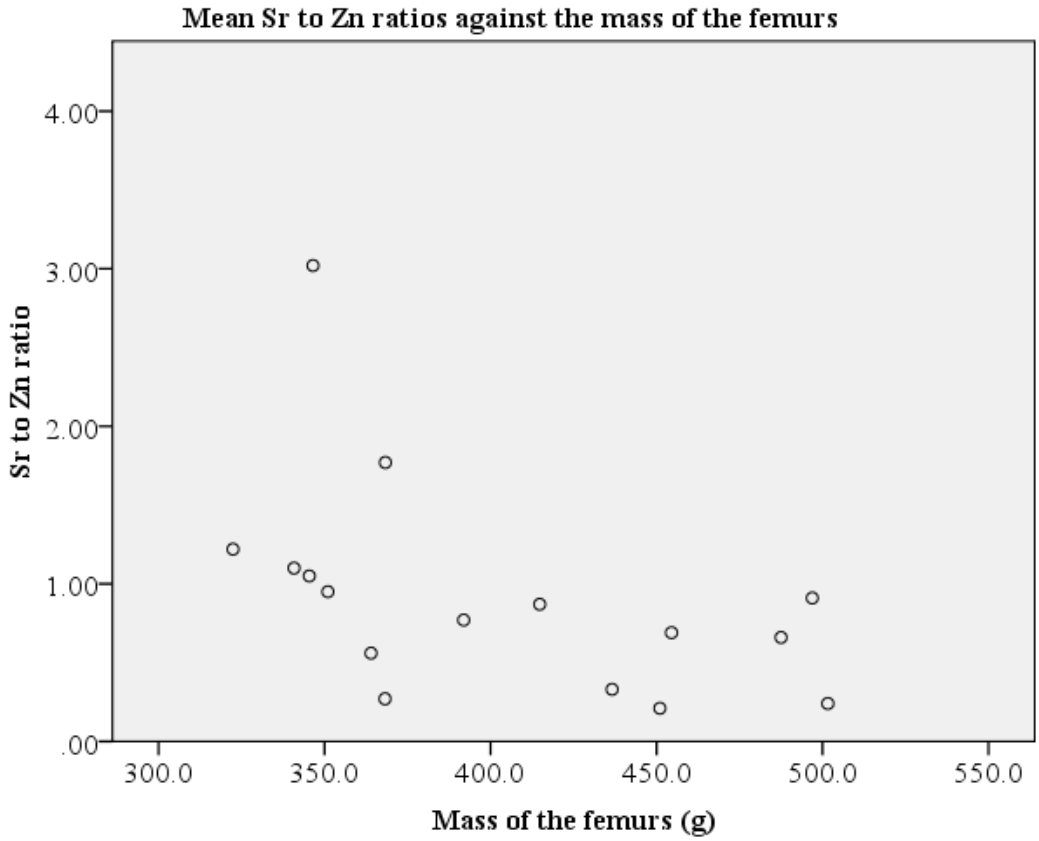

Figure 13: Average Sr to Zn ratios versus the mass of the femurs

Regression analysis from the results plotted in figure 13 showed the following: R: 0.488, R squared: 23.8%, ANOVA F statistic: 4.383 at a 0.055 significance, standard correlation coefficient -0.488 and a t test value of -2.094 at a significance of 0.055. These showed an insignificant inverse correlation between the normalized Sr to Zn ratios and the mass of the femurs. To the best of the literature review, there were no direct comparative studies in this area. These findings imply that the Sr to Zn ratio did not depend on the mass of the femurs and as such, incidences of fracture of femurs with varying masses may be based on other factors such as weight exerted on them, mechanical structure of the bones and other minerals that make up the bone matrix. Parallels can be drawn with the discussions in section 4.2.

4.4.3 Average Sr to Zn ratios and length of the femurs

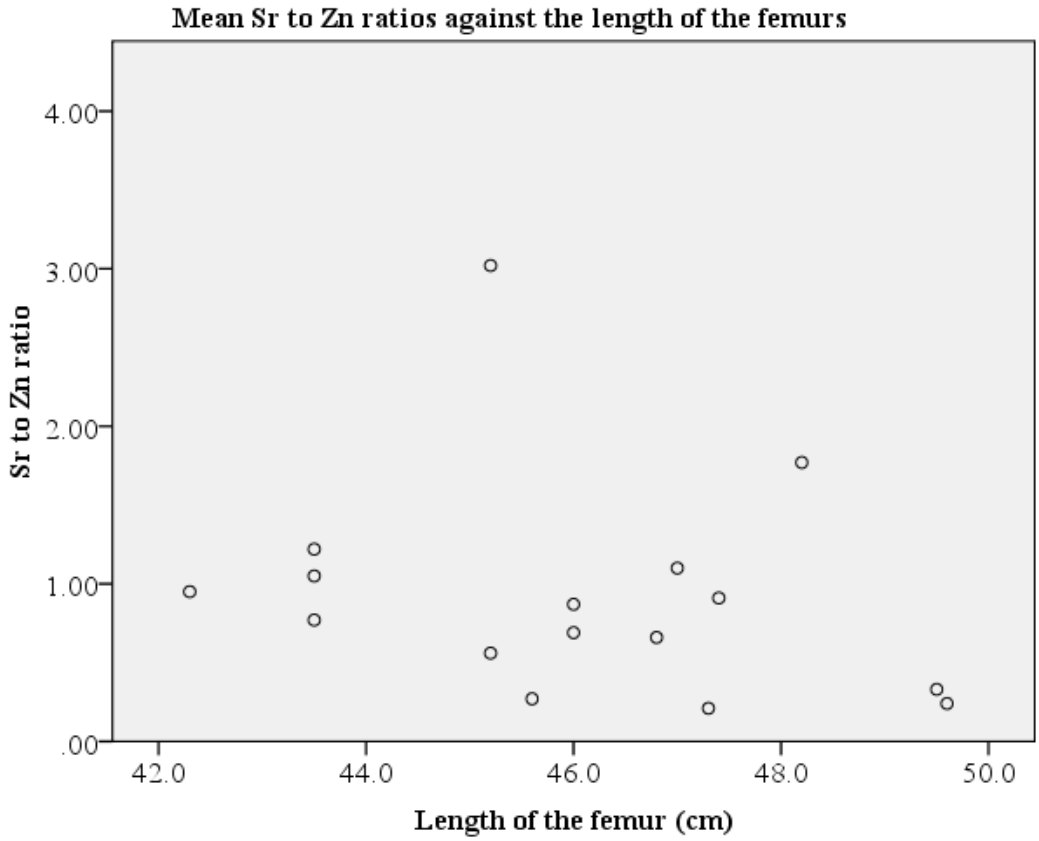

Figure 14: Average Sr to Zn ratios versus the length of the femurs

Regression analysis for the data as in figure 14 showed the following: R: 0.247, R square: 6.1%, ANOVA F test: 0.910 at a significance of 0.356, standard correlation coefficient: -0.247 and a t test value of -0.954 with a significance of 0.356 as well. These indicated an insignificant correlation between average normalized Sr to Zn ratios and the lengths of the femurs. Parallel discussions can be drawn with those in section 4.3.

4.5 Sum of Zn; Sr versus mass of the femurs

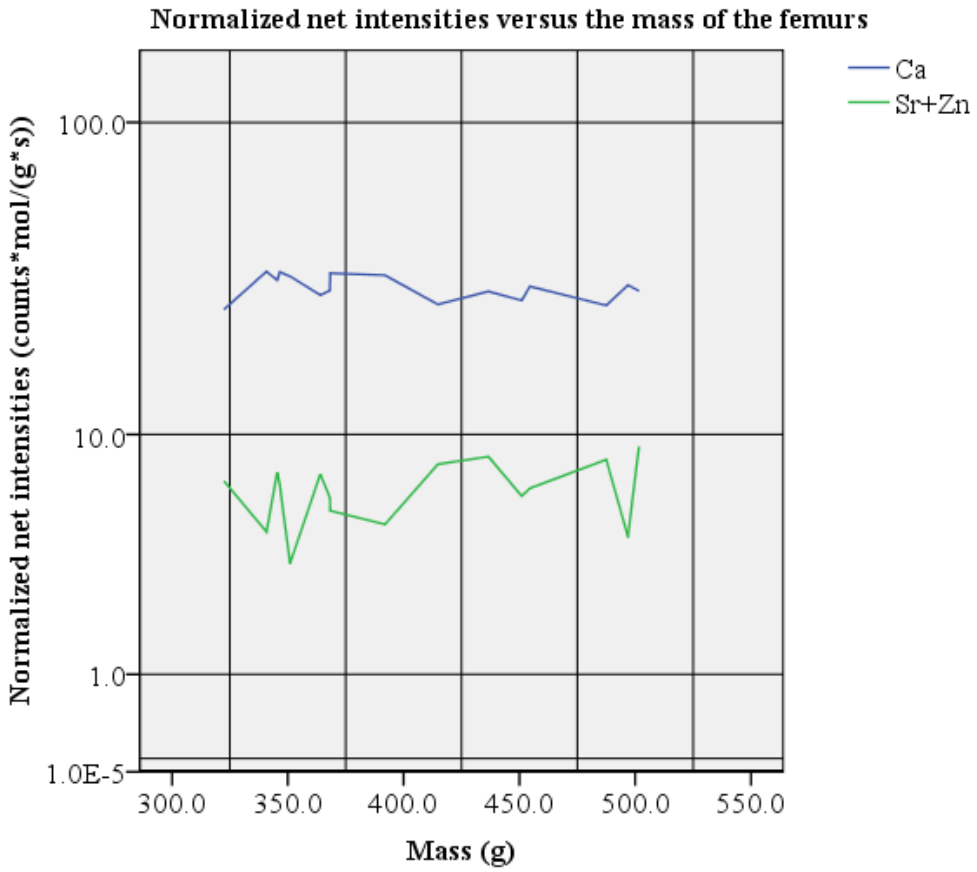

Figure 15: Normalized net intensities vs. mass of femurs

It can be seen from the graph above that, for the most part, there is an increase in the sum of Zn and Sr whenever Ca normalized net intensities are decreasing. There is also no pattern between the net intensities and the mass of the femurs. This complements observations and discussions in sections 4.1 and 4.4 of this thesis where Zn or Sr was found to be more, compared to calcium, at the cancellous regions of the femur which are normally porous. Literature review, as reported in this thesis, shows that Sr and Ca substitute each other in the bone (Pejovic et al., 2004), and in addition , compactness of the bone is associated with Ca and that Zn; Sr improve bone growth and strength respectively. Porosity of femurs, especially at their extreme

proximal and distal regions is necessary for metabolic activity within the bone which makes these regions vascular and in addition, they contain the red bone marrow from where some of the red blood cells are made (Manbachi, Hashemi, & Lashkari, 2014). This porosity makes the bone weaker and perhaps this is the reason why there is need for more Sr or Zn, at that, point so that there is improved strength without necessarily making the bone compact since both Zn and Sr have larger molar masses compared to Ca.

4.7 Sum of Zn; Sr versus length of the femurs

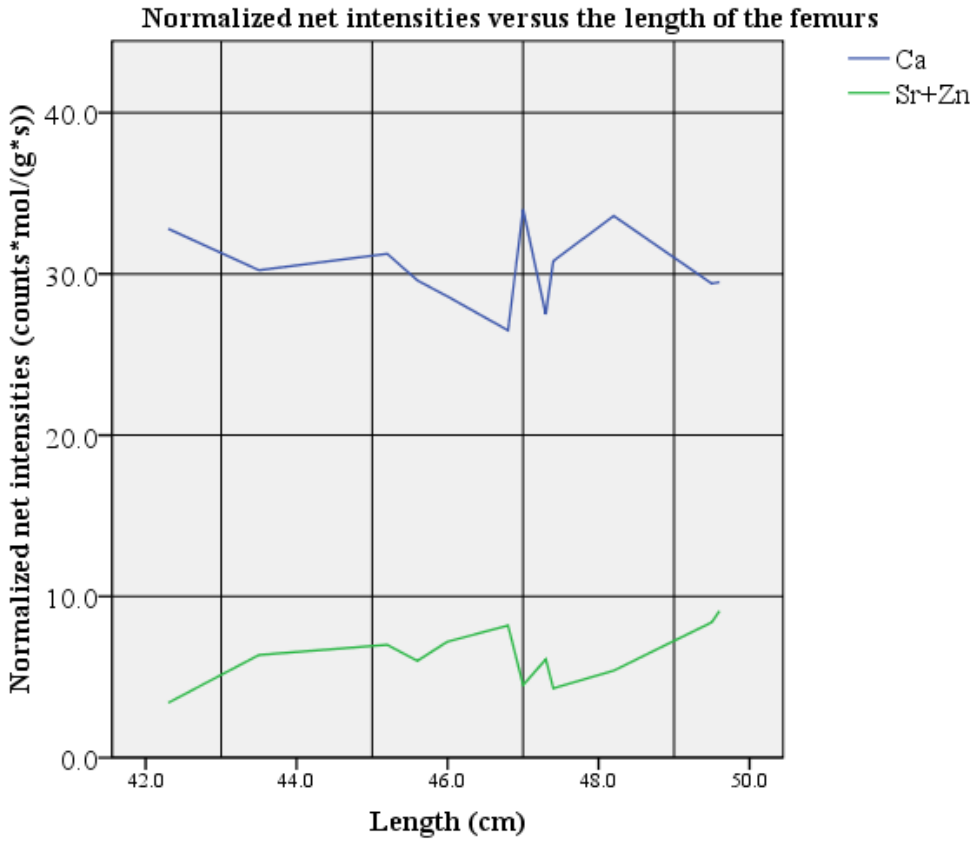

Figure 16: Normalized net intensities vs. length of femurs

The graph above shows no clear pattern between normalized net intensities and the length of the femurs. It however appears to show an inverse relationship between the

sum of Zn; Sr and Ca net intensities. Parallels can be drawn to discussions in section 4.6.

4.8 General observation

Higher relative Sr was observed at the cancellous or porous regions of the femur with the distal femur having the highest relative Sr ratios compared to the proximal femur. Additionally normalized Sr, Ca and Zn were found to be distributed across the femur in the ratio 1:12:2 respectively. There was no pattern between relative Sr and the mass or length of the femurs. It was also observed that the sum of normalized net intensities for Zn and Sr increases with decreasing Ca and vice versa.

Chapter 5

Conclusions and Recommendations

5.1 Conclusions

Distribution of normalized relative Sr, based on net intensities, appeared to depend on the region of the femur since the compact bone regions had the lowest relative Sr ratios while the cancellous bone, and more so the condyle regions, had the highest. The results show that porous regions of the bone are made stronger by incorporation of Sr or Zn which have both been associated with bone strength and bone growth stimulation. Porosity of bones was found to have a biological role even in healthy bones but this brought along mechanical weakness and hence the need by osteoblastic cells to strength them using other elements such as Sr or Zn which had higher molar masses, compared to calcium, in addition to other bone functions that have already been mentioned. Considering solid state physics, packing of smaller masses leads to compact structures with limited porosity and as such this was a probable reason as to why compact areas of the femur had more Ca compared to Zn and Sr. It can also be concluded that different regions of the femur are structurally different, perform different functions, and bear different weights hence the regional variation of relative Sr in the aforementioned pattern. The ratios of normalized Sr to Ca and Sr to Zn, based on net intensities, had no significant correlation with the mass or length of the femurs. This can probably explain why osteoporosis is found in bones regardless of their morphometric properties. Other factors such as the region of the bone, geographical site, body mass index, diet, age and physical activity of patients may account for the variations in osteoporotic cases and fractures.

5.2 Recommendations and Suggestions of further studies

It is recommended that high risk groups, such as osteoporotic patients or extreme sport participants among others, desist from engaging in physical activities that have a direct force bearing on their femoral hip axis lengths as these regions were

confirmed to be relatively weaker in this study. It is also recommended that relative Sr rich approved food substances be incorporated into diets for human consumption and non-invasive tests be done to check relative Sr in bone against the established threshold. Information on the elemental distribution along the tibia, which is also another weight bearing long bone, from the proximal to the distal end is important in ascertaining the relative Sr variation in long bones, regionally. Comparative studies can also be done with other non - weight bearing bones such as the ulna, humerus and radius. A study to compare the actual strength contribution of Sr in bone versus that of Zn may also be necessary in giving more insight into the variations of Sr and Zn in selected bones.

5.3 Limitations of the study

Femur samples obtained were neither gender nor age distinguished and this could have introduced some bias in the results considering the fact that some studies, as reported in the literature review, showed that mineral density in bones is affected by gender and age. The original study proposal intended that samples of the tibia, ulna, humerus and radius in addition to the femur be irradiated but the EDXRF system broke down resulting in the analysis of only 16 femurs. This meant that different weight bearing bones could not be compared, in terms of relative Sr distribution, to non - weight bearing ones.

Setting up the samples for irradiation would sometimes prove a challenge considering their irregular shapes, comparatively weighty nature of the femurs and the fact that there were no special sample holders for these bones other than modified supports in the form of plastics, boxes and a clamp. The likelihood of contamination from the human femurs would be high in cases were there were imperfections in the extraction of bones from the attached biological tissues during cleaning and preservation.

The study was semi quantitative in nature meaning that only the net elemental intensities could be used. This meant that only the average distribution of elements across the femurs, based on net intensities, and variations with length or mass could be studied.

5.4 De – limitations

There was a deliberate attempt to ensure that the sample selection process resulted in healthy sampled femurs free from known bone diseases and deformities. This ensured that comparisons would be possible with related studies that neither had gender nor age biases in the samples used. In as much as only sixteen femurs had been analyzed by the time the EDXRF system broke down, irradiation for 1800s had taken place for nine partitions in each of the femurs. This resulted in 144 results which would enable a statistically reliable analysis for the comparative study as in the main objective. The human bone samples were analyzed as they were after the basic cleaning and drying. This meant that sample preparation was less tedious and as such there was more focus in adjusting the fabricated sample support so as to ensure that the flattest part, of the otherwise irregular surfaced femur, rested on the source and detector volume. Prior to irradiation, the femurs had been cleaned using doubly ionized water and dried using a hot air blower which might have reduced the likelihood of biohazards from non-heat resistant pathogens.

List of References

Ahlmann, E., Patzakis, M., Roidis, N., Shepherd, L., & Holtom, P. (2002). Comparison of anterior and posterior iliac crest bone grafts in terms of harvest-site morbidity and functional outcomes. *The Journal of bone & joint surgery, 84*(5), 716-720.

Aitken, J. (1976). Factors affecting the distribution of zinc in the human skeleton. *Calcified tissue research, 20*(1), 23-30.

Alekel, D., Mortillaro, E., Hussain, E., West, B., Ahmed, N., Peterson, C., Werner, R., Arjmandi, B., & Kukreja, S. (1999). Lifestyle and biologic contributors to proximal femur bone mineral density and hip axis length in two distinct ethnic groups of premenopausal women. *Osteoporosis international, 9*(4), 327-338.

Alexander, G. V., & Nusbaum, R. E. (1959). The relative retention of strontium and calcium in human bone tissue. *Journal of Biological Chemistry (US), 234*.

Alexander, G. V., Nusbaum, R. E., & MacDonald, N. S. (1956). The relative retention of strontium and calcium in bone tissue. *Journal of Biological Chemistry, 218*, 911-919.

Bayraktar, H. H., Morgan, E. F., Niebur, G. L., Morris, G. E., Wong, E. K., & Keaveny, T. M. (2004). Comparison of the elastic and yield properties of human femoral trabecular and cortical bone tissue. *Journal of biomechanics, 37*(1), 27-35.

Bentley, R. A. (2006). Strontium isotopes from the earth to the archaeological skeleton: a review. *Journal of archaeological method and theory, 13*(3), 135-187.

Berger, C., Goltzman, D., Langsetmo, L., Joseph, L., Jackson, S., Kreiger, N., Tenenhouse, A., Davison, K. S., Josse, R. G., & Prior, J. C. (2010). Peak bone mass from longitudinal data: implications for the prevalence, pathophysiology, and diagnosis of osteoporosis. *Journal of Bone and Mineral Research, 25*(9), 1948-1957.

Cesareo, R., Napolitano, C., & Iozzino, M. (2010). Strontium ranelate in postmenopausal osteoporosis treatment: a critical appraisal. *International journal of women's health, 2*, 1.

Cohen, A., Dempster, D., Müller, R., Guo, X., Nickolas, T., Liu, X., Zhang, X., Wirth, A., Van Lenthe, G., & Kohler, T. (2010). Assessment of trabecular and cortical architecture and mechanical competence of bone by high-resolution peripheral computed tomography: comparison with transiliac bone biopsy. *Osteoporosis international, 21*(2), 263-273.

Cooper, C., Campion, G., & Melton, L. J. (1992). Hip fractures in the elderly: a world-wide projection. *Osteoporosis international, 2*(6), 285-289.

Crabtree, N., Lunt, M., Holt, G., Kroger, H., Burger, H., Grazio, S., Khaw, K.-T., Lorenc, R., Nijs, J., & Stepan, J. (2000). Hip geometry, bone mineral distribution, and bone strength in European men and women: the EPOS study. *Bone, 27*(1), 151-159.

Cvijetić Avdagić, S., Colić Barić, I., Keser, I., Cecić, I., Šatalić, Z., Bobić, J., & Gomzi, M. (2009). Differences in peak bone density between male and female students. *Arhiv za higijenu rada i toksikologiju, 60*(1), 79-86.

Dahl, S., Allain, P., Marie, P., Mauras, Y., Boivin, G., Ammann, P., Tsouderos, Y., Delmas, P., & Christiansen, C. (2001). Incorporation and distribution of strontium in bone. *Bone, 28*(4), 446-453.

Dell, R. B., Holleran, S., & Ramakrishnan, R. (2002). Sample size determination. *Ilar Journal, 43*(4), 207-213.

Doublier, A., Farlay, D., Khebbab, M. T., Jaurand, X., Meunier, P. J., & Boivin, G. (2011). Distribution of strontium and mineralization in iliac bone biopsies from osteoporotic women treated long-term with strontium ranelate. *European Journal of Endocrinology, 165*(3), 469-476.

Education Portal. (2015). Cancellous Bone: Definition, Structure & Function Retrieved 28 January, 2015, from http://education-portal.com/academy/lesson/cancellous-bone-definition-structure-function.html

Fawzy, T., Muttappallymyalil, J., Sreedharan, J., Ahmed, A., Alshamsi, S. O. S., Al Ali, M. S. S. H. B. B., & Al Balsooshi, K. A. (2011). Association between body mass index and bone mineral density in patients referred for dual-energy x-ray absorptiometry scan in Ajman, UAE. *Journal of osteoporosis, 2011*.

Felson, D. T., Zhang, Y., Hannan, M. T., & Anderson, J. J. (1993). Effects of weight and body mass index on bone mineral density in men and women: the Framingham study. *Journal of Bone and Mineral Research, 8*(5), 567-573.

Flynn, A. (2003). The role of dietary calcium in bone health. *Proceedings of the Nutrition Society, 62*(04), 851-858.

Fries, J. F., Spitz, P., Kraines, R. G., & Holman, H. R. (1980). Measurement of patient outcome in arthritis. *Arthritis & Rheumatism, 23*(2), 137-145.

Fullerton, L. R., & Snowdy, H. A. (1988). Femoral neck stress fractures. *The American journal of sports medicine, 16*(4), 365-377.

Gedalia, I. (1975). Strontium uptake by the developing femur bone and deciduous dentition. *Journal of Dental Research, 54*(2 suppl), B125.

Goh, J. C., Low, S. L., & DasDe, S. (2005). Bone mineral density and hip axis length in Singapore's multiracial population. *Journal of Clinical Densitometry, 7*(4), 406-412.

Guénin, S., Mauriat, M., Pelloux, J., Van Wuytswinkel, O., Bellini, C., & Gutierrez, L. (2009). Normalization of qRT-PCR data: the necessity of adopting a systematic, experimental conditions-specific, validation of references. *Journal of experimental botany, 60*(2), 487-493.

Gullion, C. M., Devous Sr, M. D., & Rush, A. J. (1996). Effects of four normalizing methods on data analytic results in functional brain imaging. *Biological psychiatry, 40*(11), 1106-1121.

Hammersley, J. M., Handscomb, D. C., & Weiss, G. (1965). Monte carlo methods. *Physics today, 18*, 55.

Huiskes, R., Ruimerman, R., Van Lenthe, G. H., & Janssen, J. D. (2000). Effects of mechanical forces on maintenance and adaptation of form in trabecular bone. *Nature*, *405*(6787), 704-706.

Isaacs, A. (1996). Oxford dictionary of physics. *Oxford University Press. Oxford, New-York. 474 pp., ISBN 0-19-280030-2*, *1*.

Johnson, A., Armstrong, W., & Singer, L. (1968). The incorporation and removal of large amounts of strontium by physiologic mechanisms in mineralized tissues of the rat. *Calcified tissue research*, *2*(1), 242-252.

Jordan, K., & Cooper, C. (2002). Epidemiology of osteoporosis. *Best Practice & Research Clinical Rheumatology*, *16*(5), 795-806.

Kamau, E. (2011). *Osteoporosis in the elderly, pharmacological and non pharmacological prevention and treatment (Unpublished masters thesis)*. Applied Sciences. ARCADA, Helsinki, Sweden.

Kanis, J. A., Melton, L. J., Christiansen, C., Johnston, C. C., & Khaltaev, N. (1994). The diagnosis of osteoporosis. *Journal of Bone and Mineral Research*, *9*(8), 1137-1141.

Kent, M. (2006). *The Oxford dictionary of sports science and medicine*: Oxford University Press New York, NY, USA.

Khodadadyan-Klostermann, C., von Seebach, M., Taylor, W. R., Duda, G. N., & Haas, N. P. (2004). Distribution of bone mineral density with age and gender in the proximal tibia. *Clinical Biomechanics*, *19*(4), 370-376.

Kirkpatrick, R. J. (1981). Kinetics of crystallization of igneous rocks. *Rev. Mineral.;(United States)*, *8*.

Lambert, J. B., Simpson, S. V., Buikstra, J. E., & Hanson, D. (1983). Electron microprobe analysis of elemental distribution in excavated human femurs. *American journal of physical anthropology, 62*(4), 409-423.

Landsmeer, J. (1949). The anatomy of the dorsal aponeurosis of the human finger and its functional significance. *The Anatomical Record, 104*(1), 31-44.

Lanyon, L. (1992). The success and failure of the adaptive response to functional load-bearing in averting bone fracture. *Bone, 13*, S17-S21.

Lenart, B. A., Lorich, D. G., & Lane, J. M. (2008). Atypical fractures of the femoral diaphysis in postmenopausal women taking alendronate. *New England Journal of Medicine, 358*(12), 1304-1306.

Lim, D., Golovan, S., Forsberg, C. W., & Jia, Z. (2000). Crystal structures of Escherichia coli phytase and its complex with phytate. *Nature Structural & Molecular Biology, 7*(2), 108-113.

Manbachi, A., Hashemi, S., & Lashkari, B. (2014). On estimating the directionality distribution in pedicle trabecular bone from micro-CT images. *Physiological measurement, 35*(12), 2415.

Manninger, J., & Kazár, G. (2007). Proximal Femur Fractures. Definition, Epidemiology, Anatomy, Biomechanics *Internal fixation of femoral neck fractures* (pp. 1-27): Springer.

Markowicz, A. A., & Van Grieken, R. E. (2002). *Handbook of X-ray Spectrometry*. 270 Madison Avenue, New York, USA: Marcel Dekker, Inc.

Meunier, P. J., Roux, C., Seeman, E., Ortolani, S., Badurski, J. E., Spector, T. D., Cannata, J., Balogh, A., Lemmel, E. M., & Pors-Nielsen, S. (2004). The

effects of strontium ranelate on the risk of vertebral fracture in women with postmenopausal osteoporosis. *New England Journal of Medicine, 350*(5), 459-468.

Moffat, K. L., Sun, W.-H. S., Pena, P. E., Chahine, N. O., Doty, S. B., Ateshian, G. A., Hung, C. T., & Lu, H. H. (2008). Characterization of the structure–function relationship at the ligament-to-bone interface. *Proceedings of the National Academy of Sciences, 105*(23), 7947-7952.

Molokwu, C. O., & Li, Y. V. (2006). Zinc homeostasis and bone mineral density. *Obio Research and Clinical Review, Fall, 15*, 7-15.

Nielsen, P. (2004). The biological role of strontium. *Bone, 35*(3), 583-588.

Nilsson, K., Jensen, B., & Carlsen, L. (1985). The migration chemistry of strontium. *EUR. APPL. RES. REP., 7*(1), 149-200.

Nissen, N., Hauge, E. M., Abrahamsen, B., Jensen, J.-E. B., Mosekilde, L., & Brixen, K. (2005). Geometry of the proximal femur in relation to age and sex: a cross-sectional study in healthy adult Danes. *Acta Radiologica, 46*(5), 514-518.

Pagano, A. R., Yasuda, K., Roneker, K. R., Crenshaw, T. D., & Lei, X. G. (2007). Supplemental Escherichia coli phytase and strontium enhance bone strength of young pigs fed a phosphorus-adequate diet. *The Journal of nutrition, 137*(7), 1795.

Parfitt, A. (1990). Osteomalacia and related disorders. *Metabolic bone disease and clinically related disorders. 2nd ed. Philadelphia: WB Saunders*, 329-396.

Pejovic, M., Stronach, I., Gyorffy, J., Webber, C., & Chettle, D. (2004). Quantification of bone strontium levels in humans by in vivo x-ray fluorescence. *Medical Physics, 31*, 528.

Pines, B., & Lederer, M. (1947). Osteopetrosis: Albers-Schönberg Disease (Marble Bones): Report of a Case and Morphologic Study*. *The American Journal of Pathology*, *23*(5), 755.

Plancher, K. D., & Donshik, J. D. (1997). Femoral neck and ipsilateral neck and shaft fractures in the young adult. *Orthopedic Clinics of North America, 28*(3), 447-459.

Reed, S. J. B. (1997). Electron microprobe analysis. *Electron Microprobe Analysis, by SJB Reed, Cambridge, UK: Cambridge University Press, 1997, 1*.

Reginster, J. (2002). Strontium ranelate in osteoporosis. *Current pharmaceutical design, 8*(21), 1907-1916.

Reginster, J. Y., Seeman, E., De Vernejoul, M., Adami, S., Compston, J., Phenekos, C., Devogelaer, J., Curiel, M. D., Sawicki, A., & Goemaere, S. (2005). Strontium ranelate reduces the risk of nonvertebral fractures in postmenopausal women with osteoporosis: Treatment of Peripheral Osteoporosis (TROPOS) study. *Journal of Clinical Endocrinology & Metabolism, 90*(5), 2816.

Reza, S., Rahman, M., Hossain, S., & Afroz, S. (2008). Bone mineral densities in normal Bangladeshi women. *Iranian Journal of Radiation Research, 6*(3), 157-160.

Rieke, G., Young, E., Engelbracht, C., Kelly, D., Low, F., Haller, E., Beeman, J., Gordon, K., Stansberry, J., & Misselt, K. (2004). The multiband imaging photometer for Spitzer (MIPS). *The Astrophysical Journal Supplement Series*, *154*(1), 25.

Rudman, K., Aspden, R., & Meakin, J. (2006). Compression or tension? The stress distribution in the proximal femur. *Biomed Eng Online*, *5*(2), 12.

Saloman, E., Hubbell, J., & Scofield, J. (1988). X-ray attenuation cross sections for energies 100 eV to 100 keV and elements< i> Z</i>= 1 to< i> Z</i>= 92. *Atomic Data and Nuclear Data Tables*, *38*(1), 1-196.

Schwartz, A., Kelsey, J., Maggi, S., Tuttleman, M., Ho, S., Jonsson, P., Poor, G., Sisson de Castro, J., Xu, L., & Matkin, C. (1999). International variation in the incidence of hip fractures: cross-national project on osteoporosis for the World Health Organization Program for Research on Aging. *Osteoporosis international*, *9*(3), 242-253.

Serway, R., & Vuille, C. (2015). *College physics*. Stamford, USA: Cengage Learning.

Sievänen, H., Oja, P., & Vuori, I. (1992). Precision of dual-energy x-ray absorptiometry in determining bone mineral density and content of various skeletal sites. *Journal of nuclear medicine: official publication, Society of Nuclear Medicine*, *33*(6), 1137-1142.

Silverstein, J., Moeller, J., & Hutchinson, M. (2011). Common issues in orthopedics. *Textbook of Family Medicine. 8th ed. Philadelphia, Pa: Saunders Elsevier*.

Stewart-Williams, S., & Podd, J. (2004). The placebo effect: dissolving the expectancy versus conditioning debate. *Psychological bulletin, 130*(2), 324.

Suárez-Orduña, R., Rendón-Angeles, J., Lopez-Cuevas, J., & Yanagisawa, K. (2004). The conversion of mineral celestite to strontianite under alkaline hydrothermal conditions. *Journal of Physics: Condensed Matter, 16*(14), S1331.

Teitelbaum, S. L. (2000). Bone resorption by osteoclasts. *Science, 289*(5484), 1504-1508.

Theobald, T., Cauley, J., Gluer, C., Bunker, C., Ukoli, F., & Genant, H. (1998). Black-white differences in hip geometry. *Osteoporosis international, 8*(1), 61-67.

Turner, C., Liu, G., Manatunga, A., Timmerman, L., & Johnston Jr, C. (1995). Better discrimination of hip fracture using bone density, geometry and architecture. *Osteoporosis international, 5*(3), 167-173.

University of Cambridge. (2014). Structure and composition of bone Retrieved 20 Jan, 2015, from http://www.doitpoms.ac.uk/tlplib/bones/structure.php

Wada, M., Maezawa, Y., Baba, H., Shimada, S., Sasaki, S., & Nose, Y. (2001). Relationships among bone mineral densities, static alignment and dynamic load in patients with medial compartment knee osteoarthritis. *Rheumatology, 40*(5), 499-505.

Yantis, M. A., O'Toole, K. N., & Ring, P. (2009). Leech therapy. *AJN The American Journal of Nursing, 109*(4), 36-42.

Zamburlini, M., Campbell, J., de Silveira, G., Butler, R., Pejović - Milić, A., & Chettle, D. (2009). Strontium depth distribution in human bone measured by micro - PIXE. *X - Ray Spectrometry, 38*(4), 271-277.

Appendices

A1. Spectra

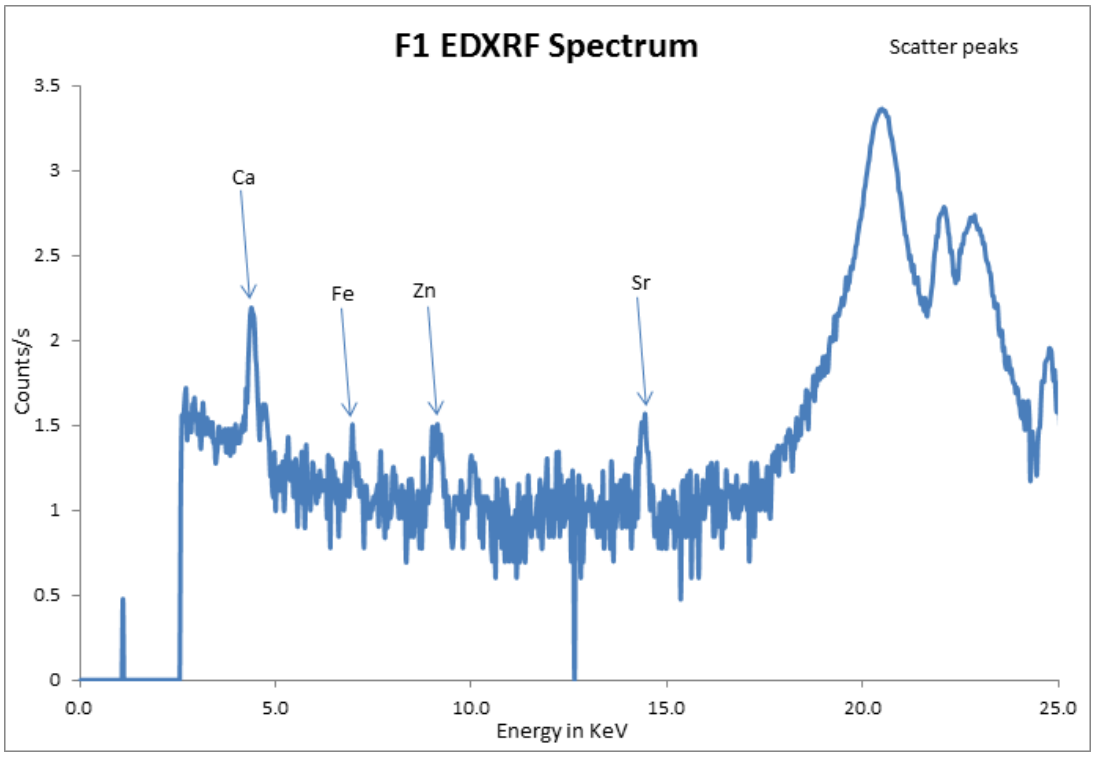

Figure 17: Femur 1 MCA spectrum

A2. Tables

These include both raw and processed data that has been used to develop graphs in chapter 4.

Table 3: Normalized elemental net intensities

b1 – b9: Irradiation point; F1 – F16: Femurs; Ca, Zn & Sr: Representative normalized net intensities $\left(\frac{counts\ s^{-1}}{gmol^{-1}}\right)$																
b1																
	F1	F2	F3	F4	F5	F6	F7	F8	F9	F10	F11	F12	F13	F14	F15	F16
Ca	12.8	35.1	17.1	17.0	17.1	28.5	13.4	28.7	34.3	17.3	27.0	23.2	30.3	36.8	27.8	23.9
Zn	3.5	4.3	7.8	2.9	2.0	3.2	4.9	6.4	2.3	1.6	1.8	2.3	0.9	2.6	1.7	2.8
Sr	1.9	2.0	3.2	2.6	2.9	1.7	0.9	1.7	2.9	1.7	1.1	2.7	4.7	2.1	2.3	1.0
b2																
Ca	22.6	33.6	17.3	24.3	30.1	28.6	21.3	29.5	29.5	21.6	38.4	28.8	23.1	36.6	40.5	19.4
Zn	2.9	15.8	4.4	2.5	2.0	0.8	4.3	5.4	2.0	2.2	2.6	2.0	0.7	2.5	1.9	3.7
Sr	2.3	1.7	2.8	2.9	3.8	1.3	1.2	2.0	1.7	2.3	3.0	3.7	4.0	2.0	3.1	1.3
b3																
Ca	31.3	25.6	30.2	33.3	18.2	32.4	28.1	20.6	27.6	30.6	34.6	29.8	34.1	26.1	32.8	30.9
Zn	2.3	2.5	3.5	2.6	0.9	1.0	1.9	7.5	1.0	2.6	1.2	2.2	1.5	1.2	2.6	3.0
Sr	2.6	1.4	3.4	4.1	2.2	1.0	0.7	1.0	1.2	1.9	5.7	3.6	3.1	2.0	2.0	1.2
b4																
Ca	30.5	28.3	31.0	34.8	24.5	33.8	29.8	29.2	32.8	29.3	35.4	28.4	35.6	30.9	34.3	32.9
Zn	6.7	5.6	4.8	3.8	1.8	1.1	4.3	6.6	2.2	5.3	2.2	3.1	1.4	3.6	2.6	5.4
Sr	2.2	1.5	2.9	4.5	2.5	1.4	0.8	1.7	2.0	1.7	3.6	3.2	3.9	2.1	2.4	1.3
b5																
Ca	24.7	35.1	29.8	32.1	35.4	32.1	33.3	26.9	33.5	34.3	33.1	34.9	37.8	35.8	33.2	31.9
Zn	8.0	9.8	4.1	5.6	3.8	1.5	4.7	7.9	2.3	8.1	1.2	5.4	1.5	3.8	2.2	4.3
Sr	1.9	1.7	3.2	4.2	3.3	1.2	0.7	1.4	1.6	2.9	2.6	3.1	5.0	1.7	2.2	1.2
b6																
Ca	33.0	25.8	24.6	28.9	26.6	32.5	30.1	32.6	25.8	35.7	36.9	32.6	37.9	33.1	32.2	26.3
Zn	7.6	7.1	4.1	4.4	7.4	1.1	5.4	7.8	3.2	6.4	2.0	4.7	2.3	3.5	3.0	4.3
Sr	2.2	1.7	2.6	3.3	3.8	1.4	0.6	2.3	1.7	2.5	3.6	3.0	4.7	2.1	1.7	1.2
b7																
Ca	26.4	21.8	28.3	20.1	20.7	31.8	25.0	32.0	33.4	32.4	28.7	32.2	23.1	26.4	24.9	29.5
Zn	6.3	5.5	4.0	4.0	4.9	2.1	3.9	6.3	2.4	6.2	1.8	5.7	1.7	2.8	1.0	4.4
Sr	1.8	1.3	3.1	2.6	3.0	1.4	0.5	1.7	2.1	2.6	2.9	2.5	3.5	1.9	1.6	1.0

b1 – b9: Irradiation point; F1 – F16: Femurs; Ca, Zn & Sr: Representative normalized net intensities $\left(\frac{counts\ s^{-1}}{gmol^{-1}}\right)$																
b8																
	F1	F2	F3	F4	F5	F6	F7	F8	F9	F10	F11	F12	F13	F14	F15	F16
Ca	34.7	30.5	27.5	24.2	16.4	40.2	30.2	30.1	29.9	34.4	35.7	38.7	46.0	37.7	35.1	37.9
Zn	4.6	5.1	5.3	7.8	3.8	5.0	8.5	11.6	4.2	3.7	4.9	8.7	4.4	4.5	2.7	8.1
Sr	2.6	1.8	2.9	3.5	2.5	2.4	1.8	1.8	2.3	2.5	2.9	4.9	8.0	1.8	2.5	1.1
b9																
Ca	41.2	29.1	33.0	25.3	42.1	35.5	35.7	36.1	30.2	38.8	33.0	38.6	37.6	34.7	45.0	33.4
Zn	3.3	4.6	7.8	7.0	5.9	1.8	8.0	7.3	1.4	2.0	1.9	2.1	2.8	1.7	2.1	7.2
Sr	2.9	2.5	4.1	3.0	5.3	1.7	1.7	2.0	2.0	2.5	3.1	3.5	6.3	1.6	2.5	1.3

Table 4: Normalized element ratios across the femurs

b1 – b9: Irradiation point; F1 – F16: Femurs; Ca, Zn & Sr: Representative normalized net intensities $\left(\frac{counts\ s^{-1}}{gmol^{-1}}\right)$																
b1																
	F1	F2	F3	F4	F5	F6	F7	F8	F9	F10	F11	F12	F13	F14	F15	F16
Ca:Sr	6.6	17.9	5.3	6.5	6.0	17.2	14.3	16.9	12.0	10.2	24.1	8.7	6.4	17.3	12.3	23.8
Ca:Zn	3.6	8.2	2.2	5.8	8.7	9.1	2.8	4.5	14.9	10.8	15.2	10.0	32.4	14.2	16.3	8.5
Zn:Sr	1.8	2.2	2.4	1.1	0.7	1.9	5.2	3.8	0.8	1.0	1.6	0.9	0.2	1.2	0.8	2.8
b2																
Ca:Sr	9.7	19.5	6.3	8.4	7.9	21.6	18.3	14.9	17.3	9.4	12.7	7.9	5.8	18.4	13.1	14.8
Ca:Zn	7.9	2.1	3.9	9.8	15.3	35.2	5.0	5.4	14.9	9.7	14.6	14.3	31.4	14.8	21.5	5.3
Zn:Sr	1.2	9.2	1.6	0.9	0.5	0.6	3.7	2.8	1.2	1.0	0.9	0.6	0.2	1.2	0.6	2.8
b3																
Ca:Sr	12.1	18.4	9.0	8.1	8.2	32.3	39.1	20.5	23.5	16.4	6.1	8.2	11.0	13.1	16.3	26.3
Ca:Zn	13.5	10.2	8.7	12.8	21.2	33.1	14.5	2.8	26.9	11.8	28.6	13.4	23.2	21.9	12.9	10.2
Zn:Sr	0.9	1.8	1.0	0.6	0.4	1.0	2.7	7.4	0.9	1.4	0.2	0.6	0.5	0.6	1.3	2.6
b4																
Ca:Sr	13.7	18.6	10.5	7.7	9.6	24.4	37.9	17.4	16.6	17.5	9.7	8.8	9.1	14.4	14.3	25.7
Ca:Zn	4.6	5.1	6.5	9.1	13.8	29.8	6.9	4.4	14.6	5.5	16.4	9.2	25.9	8.6	13.3	6.1
Zn:Sr	3.0	3.7	1.6	0.8	0.7	0.8	5.5	3.9	1.1	3.2	0.6	1.0	0.4	1.7	1.1	4.2

b5																
Ca:Sr	13.3	21.1	9.2	7.6	10.6	26.8	44.9	19.2	21.0	11.8	12.5	11.3	7.6	20.6	14.8	27.2
Ca:Zn	3.1	3.6	7.3	5.7	9.4	21.9	7.0	3.4	14.4	4.2	27.8	6.4	26.0	9.4	14.9	7.4
Zn:Sr	4.3	5.9	1.3	1.3	1.1	1.2	6.4	5.6	1.5	2.8	0.5	1.8	0.3	2.2	1.0	3.7
b6																
Ca:Sr	15.3	15.6	9.3	8.8	7.1	23.9	48.9	14.3	14.8	14.1	10.2	10.9	8.0	15.9	18.6	22.6
Ca:Zn	4.3	3.7	5.9	6.6	3.6	30.3	5.6	4.2	8.1	5.6	18.3	7.0	16.6	9.4	10.8	6.2
Zn:Sr	3.5	4.3	1.6	1.3	2.0	0.8	8.7	3.4	1.8	2.5	0.6	1.6	0.5	1.7	1.7	3.7
	F1	F2	F3	F4	F5	F6	F7	F8	F9	F10	F11	F12	F13	F14	F15	F16
b7																
Ca:Sr	14.4	16.7	9.0	7.7	6.9	23.0	49.8	18.7	15.7	12.6	10.1	12.7	6.6	14.0	15.6	29.4
Ca:Zn	4.2	4.0	7.1	5.1	4.2	14.9	6.4	5.1	13.8	5.2	15.8	5.7	13.6	9.4	24.3	6.7
Zn:Sr	3.4	4.2	1.3	1.5	1.6	1.5	7.7	3.7	1.1	2.4	0.6	2.2	0.5	1.5	0.6	4.4
b8																
	F1	F2	F3	F4	F5	F6	F7	F8	F9	F10	F11	F12	F13	F14	F15	F16
Ca:Sr	13.5	17.1	9.5	6.9	6.5	16.8	16.7	17.1	12.8	13.6	12.2	7.9	5.7	21.0	14.1	33.9
Ca:Zn	7.6	6.0	5.2	3.1	4.3	8.0	3.5	2.6	7.1	9.2	7.3	4.5	10.5	8.4	12.9	4.7
Zn:Sr	1.8	2.8	1.8	2.3	1.5	2.1	4.7	6.6	1.8	1.5	1.7	1.8	0.5	2.5	1.1	7.2
b9																
Ca:Sr	14.3	11.6	8.0	8.5	8.0	21.4	20.6	18.3	15.5	15.6	10.6	11.1	5.9	21.9	17.8	26.1
Ca:Zn	12.5	6.3	4.2	3.6	7.2	19.8	4.4	4.9	21.4	19.1	17.1	18.3	13.5	20.6	21.3	4.6
Zn:Sr	1.1	1.8	1.9	2.4	1.1	1.1	4.6	3.7	0.7	0.8	0.6	0.6	0.4	1.1	0.8	5.6

Table 5: Sr:Ca ratios across the femurs - Analyzed figures with reduced standard deviation

Sr:Ca	b1	b2	b3	b4	b5	b6	b7	b8	b9
F1	1.79	1.21	0.97	0.86	0.89	0.77	0.82	0.87	0.82
F2	0.95	0.87	0.92	0.91	0.80	1.09	1.01	0.99	1.46
F3	1.52	1.29	0.90	0.77	0.88	0.87	0.90	0.85	1.01
F4	1.19	0.92	0.95	1.00	1.02	0.88	1.00	1.12	0.91
F5	1.27	0.97	0.93	0.79	0.72	1.08	1.11	1.17	0.96
F6	1.29	1.03	0.69	0.91	0.83	0.93	0.97	1.32	1.04
F7	1.80	1.41	0.66	0.68	0.58	0.53	0.52	1.55	1.26
F8	1.02	1.16	0.84	0.99	0.90	1.21	0.92	1.01	0.94

Sr:Ca	b1	b2	b3	b4	b5	b6	b7	b8	b9
F9	1.33	0.92	0.68	0.96	0.76	1.08	1.01	1.24	1.03
F10	1.26	1.38	0.79	0.74	1.09	0.92	1.03	0.95	0.83
F11	0.44	0.84	1.76	1.10	0.86	1.05	1.06	0.88	1.01
F12	1.09	1.20	1.15	1.07	0.84	0.87	0.74	1.20	0.85
F13	1.10	1.22	0.64	0.77	0.93	0.87	1.06	1.22	1.19
F14	0.97	0.92	1.28	1.17	0.82	1.06	1.20	0.80	0.77
F15	1.22	1.14	0.92	1.05	1.01	0.80	0.96	1.06	0.84
F16	1.02	1.65	0.93	0.95	0.90	1.08	0.83	0.72	0.93
Average	1.20	1.13	0.94	0.92	0.86	0.94	0.95	1.06	0.99
SD	0.33	0.23	0.28	0.14	0.12	0.17	0.16	0.22	0.18

SD: Standard Deviation

Table 6: Bivariate correlations of Sr to Ca ratios for normalized intensity values across the 16 femurs

	Pearson Correlations (N = 16)								
	b1	b2	b3	b4	b5	b6	b7	b8	b9
b1	1.0								
b2	0.9	1.0							
b3	0.5	0.6	1.0						
b4	0.7	0.8	0.9	1.0					
b5	0.8	0.9	0.7	0.9	1.0				
b6	0.7	0.8	0.8	0.9	0.9	1.0			
b7	0.7	0.8	0.8	0.9	0.9	1.0	1.0		
b8	0.8	0.8	0.6	0.8	0.9	0.9	0.9	1.0	
b9	0.7	0.9	0.7	0.8	0.9	0.9	0.9	0.9	1.0

	Red: Correlation is significant at the 0.01 level (2-tailed).
	Blue: Correlation is significant at the 0.05 level (2-tailed).

Table 7: Sample SPSS regression analysis output

Model Summary

Model	R	R Square	Adjusted R Square	Std. Error of the Estimate
1	.252[a]	.063	-.004	.034587

a. Predictors: (Constant), Mass of the femur (g)

ANOVA[b]

Model		Sum of Squares	df	Mean Square	F	Sig.
1	Regression	.001	1	.001	.947	.347[a]
	Residual	.017	14	.001		
	Total	.018	15			

a. Predictors: (Constant), Mass of the femur (g)

b. Dependent Variable: Sr to Ca ratio

Coefficients[a]

Model		Unstandardized Coefficients		Standardized Coefficients	t	Sig.
		B	Std. Error	Beta		
1	(Constant)	.140	.060		2.342	.034
	Mass of the femur (g)	.000	.000	-.252	-.973	.347

a. Dependent Variable: Sr to Ca ratio

Table 8: Sr:Zn ratios across the femurs - Analyzed figures with reduced standard deviation

Sr:Zn	b1	b2	b3	b4	b5	b6	b7	b8	b9
F1	0.98	1.45	1.98	0.59	0.41	0.51	0.52	1.00	1.56
F2	1.41	0.33	1.70	0.83	0.52	0.72	0.73	1.08	1.67
F3	0.63	0.95	1.48	0.94	1.21	0.97	1.19	0.83	0.80
F4	1.02	1.34	1.81	1.36	0.86	0.86	0.75	0.51	0.49
F5	1.19	1.59	2.12	1.18	0.73	0.42	0.50	0.54	0.74
F6	0.55	1.72	1.08	1.29	0.86	1.34	0.68	0.50	0.97
F7	0.94	1.33	1.80	0.88	0.76	0.56	0.63	1.04	1.05
F8	1.10	1.50	0.55	1.05	0.73	1.20	1.13	0.62	1.11
F9	1.36	0.95	1.26	0.97	0.76	0.61	0.97	0.61	1.52
F10	1.53	1.51	1.05	0.46	0.52	0.58	0.60	0.98	1.78
F11	0.36	0.65	2.65	0.95	1.25	1.01	0.88	0.34	0.91
F12	1.09	1.72	1.54	0.99	0.54	0.61	0.42	0.54	1.56
F13	1.68	1.80	0.70	0.94	1.14	0.68	0.68	0.61	0.76
F14	1.06	1.04	2.15	0.78	0.59	0.77	0.87	0.52	1.22
F15	1.20	1.48	0.72	0.84	0.91	0.52	1.41	0.83	1.09
F16	1.32	1.32	1.43	0.88	1.01	1.01	0.85	0.51	0.66
Average	1.09	1.29	1.50	0.93	0.80	0.77	0.80	0.69	1.12
SD	0.35	0.41	0.59	0.23	0.26	0.27	0.27	0.23	0.40

Table 9: Bivariate correlations of Sr to Zn ratios for normalized intensity values across the femurs

	Pearson Correlations (N=16)								
	b1	b2	b3	b4	b5	b6	b7	b8	b9
b1	1.0								
b2	1.0	1.0							
b3	0.3	0.4	1.0						
b4	0.8	0.9	0.7	1.0					
b5	0.8	0.9	0.7	0.9	1.0				
b6	0.7	0.8	0.7	0.9	0.9	1.0			
b7	0.7	0.7	0.6	0.8	0.9	0.8	1.0		
b8	0.9	0.9	0.4	0.8	0.8	0.7	0.8	1.0	
b9	0.7	0.8	0.6	0.8	0.8	0.7	0.8	0.8	1.0
	Red: Correlation is significant at the 0.01 level (2-tailed).								
	Blue: Correlation is significant at the 0.05 level (2-tailed).								

Table 10: Morphometric properties vs. normalized net intensities

Femur	Mass (g)	Length (cm)	Normalized	
			Zn+Sr	Ca
1	364.0	45.2	7.3	28.6
2	436.6	49.5	8.4	29.4
3	487.5	46.8	8.2	26.5
4	414.8	46.0	7.9	26.7
5	322.4	43.5	6.9	25.7
6	351.0	42.3	3.4	32.8
7	451.0	47.3	6.1	27.5
8	501.6	49.6	9.1	29.5
9	496.9	47.4	4.3	30.8
10	454.5	46.0	6.5	30.5
11	368.3	48.2	5.4	33.6
12	345.4	43.5	7.4	31.9
13	346.5	45.2	6.7	33.9
14	391.9	43.5	4.8	33.1
15	340.8	47.0	4.5	34.0
16	368.2	45.6	6.0	29.6

A2. Additional results and analysis

A2.1 Correlation between length and mass of the femurs

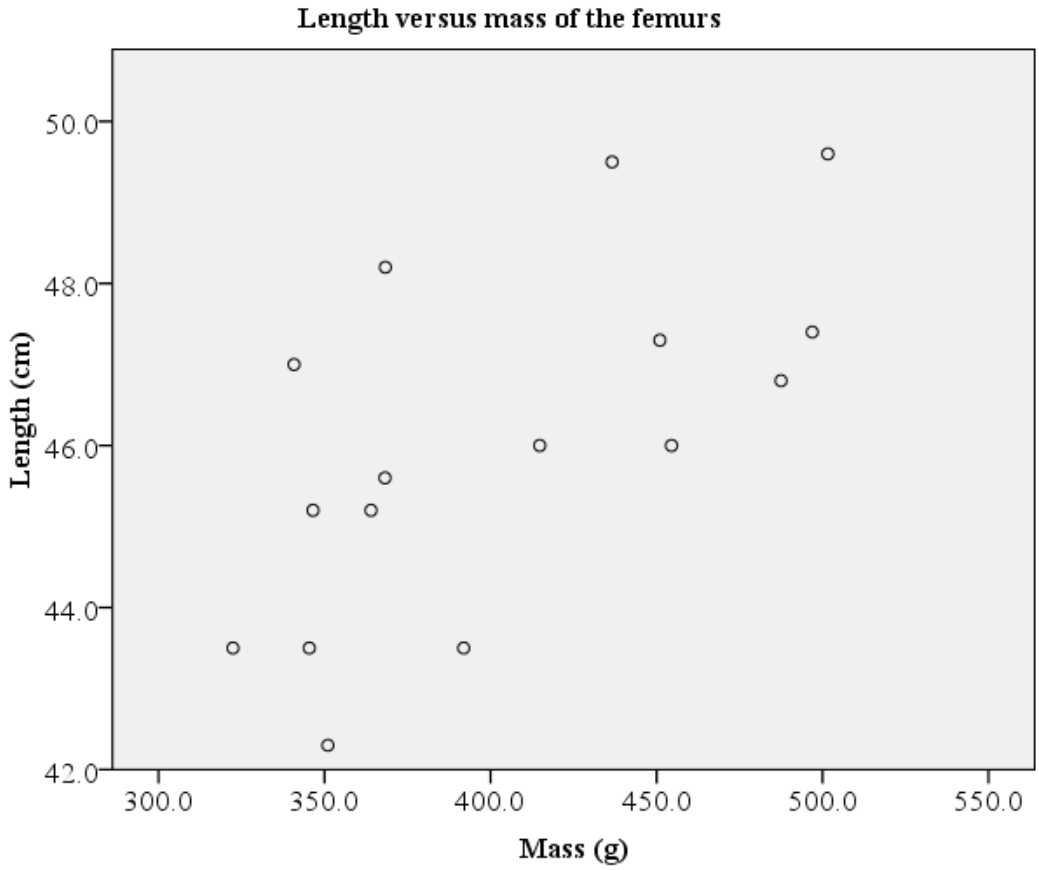

Figure 18: Length vs mass of femurs

A2.2 Average normalized Zn to Ca ratios versus mass of the femurs

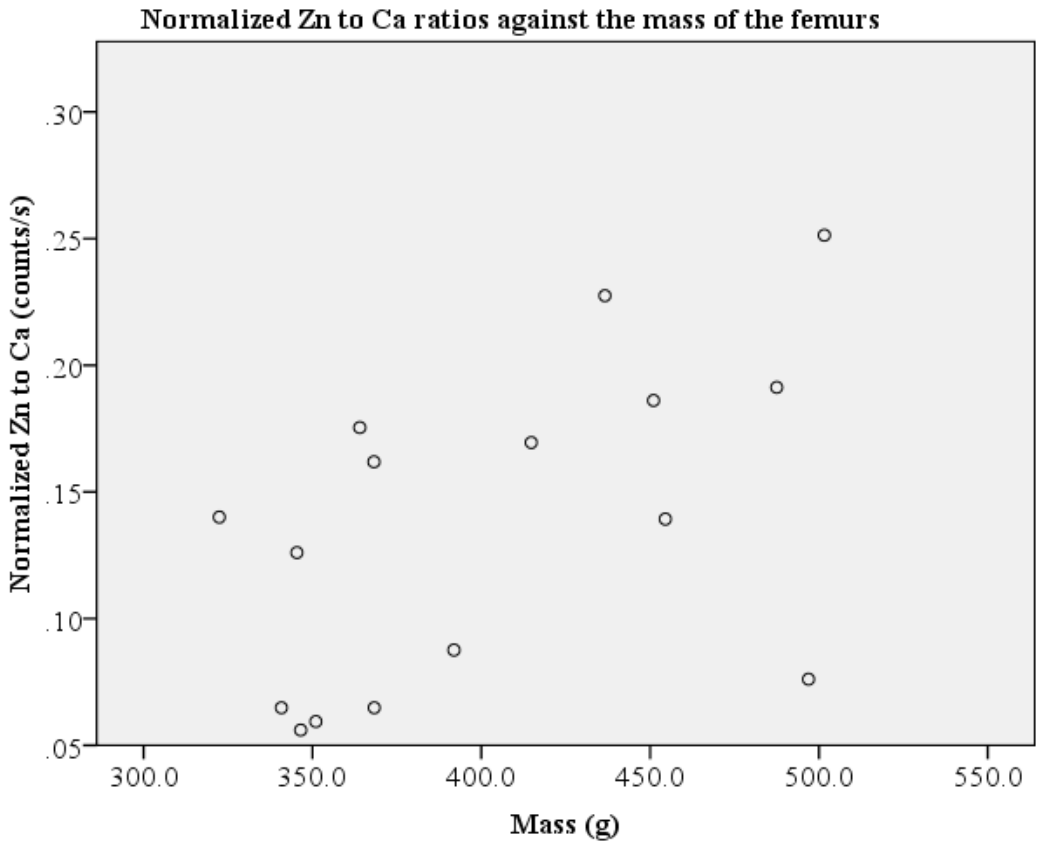

Figure 19: Zn:Ca vs femur mass

A2.3 Average normalized Zn and the mass of the femurs

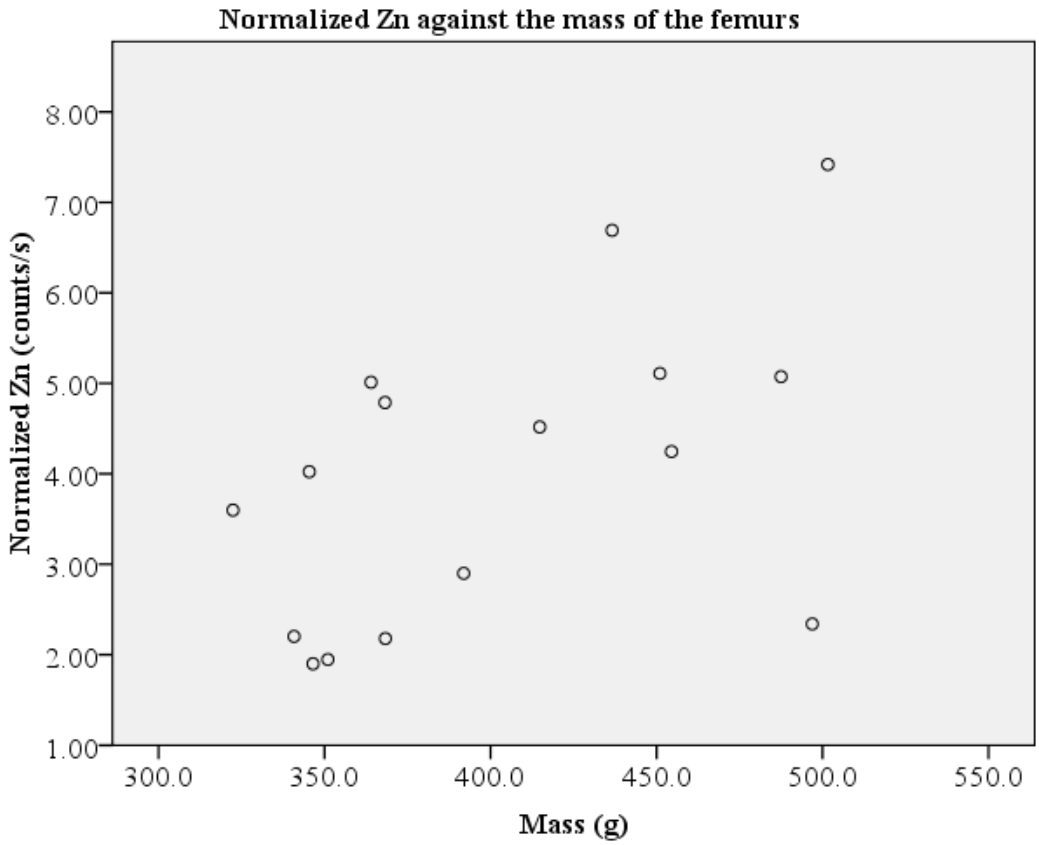

Figure 20: Average Zn vs mass of the femurs

A2.4 Average normalized Zn and length of femur

Figure 21: Normalized Zn vs femur length